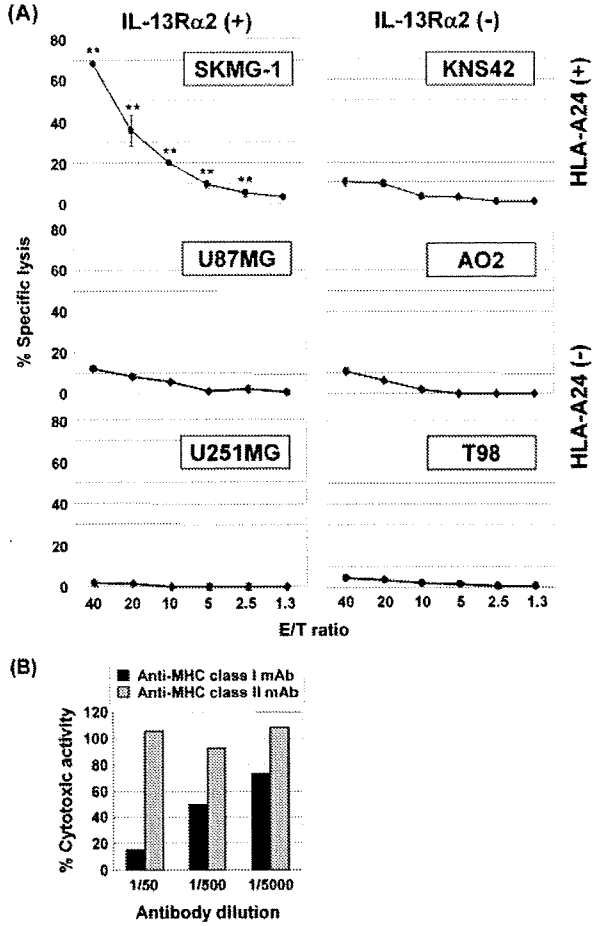

FIG. 4. Graphs demonstrating the specificity of P174-induced CTL line. A: Cytotoxic activity of P174-induced CTLs against various glioma cell lines. The cytotoxic activity of P174-induced CTLs was tested using the standard 4-hour ^{51}Cr release assay to confirm their HLA restriction and antigen specificity. Results are shown as the means ± standard deviations. **The lytic activity of P174-induced CTLs against the SKMG-1 cell line at the E/T ratio is significantly different than those against the other glioma cell lines ($p < 0.05$). B: Bar graph demonstrating the antibody blocking assay. The cytotoxic activity of P174-induced CTLs was tested using the standard 4-hour ^{51}Cr release assay in the presence or absence of anti–MHC Class I or Class II monoclonal antibody (mAb); SKMG-1 cells were the target. The results are expressed in terms of percent specific activity, and cytotoxicity without monoclonal antibodies is defined as 100%.

Substantial time and effort in the laboratory is generally required to identify new CTL epitopes. To improve the identification process, online bioinformatics algorithms are commonly used to predict which epitope will bind to a particular HLA. There are some algorithms available on the internet that use a scoring system to predict the binding affinity of a given peptide,[19] and we selected 5 peptides for this study using the BIMAS algorithm. We also performed an MHC stabilization assay to evaluate each peptide's affinity for the HLA-A24 molecule.[13] The results of our MHC stabilizing assay showed that P146, which had the third highest score on BIMAS analysis, has the greatest affinity for the HLA-A24 molecule. In generating CTLs from DCs pulsed with the candidate peptides, we found that the

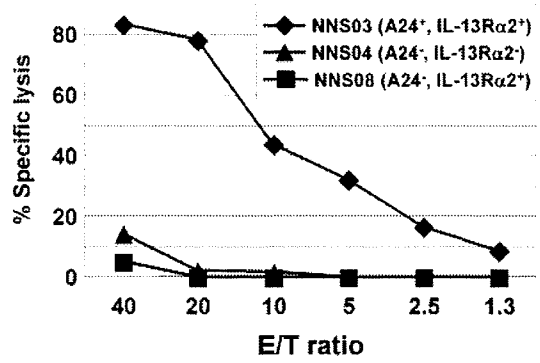

FIG. 5. Graph demonstrating cytotoxicity of P174-induced CTLs against primary-cultured glioma cells from surgically removed tissues. The cytotoxic activity of P174-induced CTLs was tested using the standard 4-hour ^{51}Cr release assay.

P174 peptide was the most potent epitope and induced CTLs with a fine-tuned specificity to IL-13Rα2 and HLA-A24. However, this result appears to be inconsistent with those of the MHC stabilization assay because the P146-derived CTLs were less efficient in causing lysis in the SKMG-1 cells. Proteasomal cleavage of the mother protein is an important process for antigen presentation by MHC Class I molecules, and we speculate that the sequences of the predicted antigenic peptides are not always in accordance with the predicted proteasome cleavage sites.[22] Based on a proteosomal cleavage site prediction system, we also confirmed that among the 5 candidates, only the ends of the P174 peptide are the cleavage sites.[17] In addition, it has been reported that peptide-binding assays might not be sufficiently sensitive to detect the binding of all natural ligands.[8] To confirm that cytotoxicity of the P174-derived CTLs is truly restricted to IL-13Rα2 and HLA-A24, we conducted CTL assays in 6 glioma cell lines that have different levels of IL-13Rα2 and HLA-A24 expression. The results showed the remarkable cell lytic activity of the P174-derived CTLs against SKMG-1 cells. The cytotoxicity observed with cells that had undergone DC stimulation 4 times was much higher (~ 70%) than that in the cells that had undergone DC stimulation 3 times (~ 35%). This indicates that repeated DC pulsation leads to an increase in the specific cytotoxicity of CTLs. This finding has also been described in a previous study,[11] and it could be speculated that the repetition of DC pulsation contributes to higher purification of the CTLs specific to the peptide. The restriction of the CTLs to both IL-13Rα2 and HLA-A24 was verified by the minimal cytotoxicity to the other 5 kinds of glioma cells, and the effective inhibition of tumor cell lysis in the presence of anti–MHC Class I antibody. In addition, it is noteworthy that the lytic activity of P174-derived CTLs against the primary glioma cells obtained from the surgical specimens was also restricted to both HLA-A24 and IL-13Rα2; this raises the possibility future application in patients.

To our knowledge, this is the first study in which a novel HLA-A24–restricted CTL epitope peptide derived from the IL-13Rα2 protein has been identified. The P174 peptide was confirmed to be the most effective in inducing $CD8^+$ CTLs to destroy glioma cells expressing both HLA-A24 and IL-13Rα2. In addition to its high prevalence in Asians,

HLA-A24 is also expressed in 17% of Caucasians, 27% of Hispanics, and 9% of African-Americans.[3] Another HLA-A allele, HLA-A2, is the most common HLA-A allele in the world, occurring in 40% of Japanese, 60% of Caucasians and Chinese, 69% of Hispanics, and 31% of African-Americans.[9] Therefore, large number of patients with gliomas all over the world would be expected to show either HLA-A24 or HLA-2 expression. Indeed in the 14 patients with gliomas who we examined for HLA typing, 7 carried the *HLA-A24* allele and 6 the *HLA-A2* allele. Coupled with an HLA-A0201–restricted peptide associated with IL-13Rα2 that has been identified,[18] the majority of gliomas could potentially be treated with immunotherapy targeting IL-13Rα2 in a peptide or DC-based vaccination.[23,24] Although our study is in its first phase and further studies are needed, our data could contribute to the development of the immunotherapy for malignant gliomas.

Conclusions

Our results demonstrate that IL-13Rα2 could be a very promising antigen for the treatment of high-grade gliomas. We first identified a novel HLA-A24–restricted CTL epitope peptide derived from the IL-13Rα2 protein using glioma cell lines and primary glioma cells. The P174 peptide could eventually provide a peptide-based immunotherapy against malignant gliomas in patients with HLA-A24 expression.

Acknowledgment

We thank Ms. Aya Murashita for her wonderful technical assistance.

References

1. Bernard J, Treton D, Vermot Desroches C, Boden C, Horellou P, Angevin E, et al: Expression of interleukin 13 receptor in glioma and renal cell carcinoma: IL13Ralpha2 as a decoy receptor for IL13. **Lab Invest 81:**1223–1231, 2001
2. Celis E, Sette A, Grey HM: Epitope selection and development of peptide based vaccines to treat cancer. **Semin Cancer Biol 6:** 329–336, 1995
3. Date Y, Kimura A, Kato H, Sasazuki T: DNA typing of the HLA-A gene: population study and identification of four new alleles in Japanese. **Tissue Antigens 47:**93–101, 1996
4. Debinski W, Gibo DM: Molecular expression analysis of restrictive receptor for interleukin 13, a brain tumor-associated cancer/testis antigen. **Mol Med 6:**440–449, 2000
5. Debinski W, Gibo DM, Hulet SW, Connor JR, Gillespie GY: Receptor for interleukin 13 is a marker and therapeutic target for human high-grade gliomas. **Clin Cancer Res 5:**985–990, 1999
6. Debinski W, Gibo DM, Slagle B, Powers SK, Gillespie GY: Receptor for interleukin 13 is abundantly and specifically over-expressed in patients with glioblastoma multiforme. **Int J Oncol 15:** 481–486, 1999
7. Debinski W, Slagle B, Gibo DM, Powers SK, Gillespie GY: Expression of a restrictive receptor for interleukin 13 is associated with glial transformation. **J Neurooncol 48:**103–111, 2000
8. Hebart H, Daginik S, Stevanovic S, Grigoleit U, Dobler A, Baur M, et al: Sensitive detection of human cytomegalovirus peptide-specific cytotoxic T-lymphocyte responses by interferon-gamma-enzyme-linked immunospot assay and flow cytometry in healthy individuals and in patients after allogeneic stem cell transplantation. **Blood 99:**3830–3837, 2002
9. Imanishi T, Akazawa T, Kimura A, Tokunaga K, Gojobori T: Allele and haplotype frequencies for HLA and complement loci in various ethnic groups, in Tsuji K, Aizawa M, Sasazuki T (eds): **HLA 1991.** New York: Oxford University Press, 1992, Vol 1, pp 1065–1220
10. Joshi BH, Plautz GE, Puri RK: Interleukin-13 receptor alpha chain: a novel tumor-associated transmembrane protein in primary explants of human malignant gliomas. **Cancer Res 60:**1168–1172, 2000
11. Kiessling A, Fussel S, Schmitz M, Stevanovic S, Meye A, Weigle B, et al: Identification of an HLA-A*0201-restricted T-cell epitope derived from the prostate cancer-associated protein trp-p8. **Prostate 56:**270–279, 2003
12. Kioi M, Kawakami M, Shimamura T, Husain SR, Puri RK: Interleukin-13 receptor alpha2 chain: a potential biomarker and molecular target for ovarian cancer therapy. **Cancer 107:**1407–1418, 2006
13. Kuzushima K, Hayashi N, Kimura H, Tsurumi T: Efficient identification of HLA-A*2402-restricted cytomegalovirus-specific CD8(+) T-cell epitopes by a computer algorithm and an enzyme-linked immunospot assay. **Blood 98:**1872–1881, 2001
14. Miloux B, Laurent P, Bonnin O, Lupker J, Caput D, Vita N, et al: Cloning of the human IL-13R alpha1 chain and reconstitution with the IL4R alpha of a functional IL-4/IL-13 receptor complex. **FEBS Lett 401:**163–166, 1997
15. Mintz A, Gibo DM, Madhankumar AB, Debinski W: Molecular targeting with recombinant cytotoxins of interleukin-13 receptor alpha2-expressing glioma. **J Neurooncol 64:**117–123, 2003
16. Mintz A, Gibo DM, Slagle-Webb B, Christensen ND, Debinski W: IL-13Ralpha2 is a glioma-restricted receptor for interleukin-13. **Neoplasia 4:**388–399, 2002
17. Nussbaum AK, Kuttler C, Hadeler KP, Rammensee HG, Schild H: PAProC: a prediction algorithm for proteasomal cleavages available on the WWW. **Immunogenetics 53:**87–94, 2001
18. Okano F, Storkus WJ, Chambers WH, Pollack IF, Okada H: Identification of a novel HLA-A*0201-restricted, cytotoxic T lymphocyte epitope in a human glioma-associated antigen, interleukin 13 receptor alpha2 chain. **Clin Cancer Res 8:**2851–2855, 2002
19. Rammensee H, Bachmann J, Emmerich NP, Bachor OA, Stevanovic S: SYFPEITHI: database for MHC ligands and peptide motifs. **Immunogenetics 50:**213–219, 1999
20. Rosenberg SA: Cancer vaccines based on the identification of genes encoding cancer regression antigens. **Immunol Today 18:** 175–182, 1997
21. Sikorski CW, Lesniak MS: Immunotherapy for malignant glioma: current approaches and future directions. **Neurol Res 27:**703–716, 2005
22. Tanaka K, Tanahashi N, Tsurumi C, Yokota KY, Shimbara N: Proteasomes and antigen processing. **Adv Immunol 64:**1–38, 1997
23. Yajima N, Yamanaka R, Mine T, Tsuchiya N, Homma J, Sano M, et al: Immunologic evaluation of personalized peptide vaccination for patients with advanced malignant glioma. **Clin Cancer Res 11:**5900–5911, 2005
24. Yamanaka R, Yajima N, Abe T, Tsuchiya N, Homma J, Narita M, et al: Dendritic cell-based glioma immunotherapy. **Int J Oncol 23:**5–15, 2003
25. Zurawski G, de Vries JE: Interleukin 13 elicits a subset of the activities of its close relative interleukin 4. **Stem Cells 12:**169–174, 1994
26. Zurawski SM, Vega F Jr, Huyghe B, Zurawski G: Receptors for interleukin-13 and interleukin-4 are complex and share a novel component that functions in signal transduction. **EMBO J 12:** 2663–2670, 1993

Manuscript submitted April 5, 2007.
Accepted August 29, 2007.
Address correspondence to: Jun Yoshida, M.D., Ph.D., Department of Neurosurgery, Nagoya University School of Medicine, 65 Tsurumai-cho, Showa-ward, Nagoya, Aichi, Japan 466-8550. email: nsoffice@med.nagoya-u.ac.jp.

Identification of human minor histocompatibility antigens based on genetic association with highly parallel genotyping of pooled DNA

Takakazu Kawase,[1,2] Yasuhito Nannya,[3-5] Hiroki Torikai,[1] Go Yamamoto,[3-5] Makoto Onizuka,[6] Satoko Morishima,[1] Kunio Tsujimura,[7] Koichi Miyamura,[5,8] Yoshihisa Kodera,[5,8] Yasuo Morishima,[5,9] Toshitada Takahashi,[10] Kiyotaka Kuzushima,[1] Seishi Ogawa,[3-5] and Yoshiki Akatsuka[1,5]

[1]Division of Immunology, [2]Division of Epidemiology and Prevention, Aichi Cancer Center Research Institute, Nagoya; [3]Department of Hematology/Oncology and [4]21st Century COE Program, Graduate School of Medicine, University of Tokyo, Tokyo; [5]Core Research for Evolutional Science and Technology, Japan Science and Technology Agency, Saitama; [6]Department of Genetic Information, Division of Molecular Life Science, Tokai University School of Medicine, Isehara; [7]Department of Microbiology and Immunology, Hamamatsu University School of Medicine, Hamamatsu; [8]Department of Hematology, Japanese Red Cross Nagoya First Hospital, Nagoya; [9]Department of Hematology and Cell Therapy, Aichi Cancer Center Hospital, Nagoya; and [10]Aichi Comprehensive Health Science Center, Aichi Health Promotion Foundation, Chita-gun, Japan

Minor histocompatibility (H) antigens are the molecular targets of allo-immunity responsible both for the development of antitumor effects and for graft-versus-host disease (GVHD) in allogeneic hematopoietic stem cell transplantation (allo-HSCT). However, despite their potential clinical use, our knowledge of human minor H antigens is largely limited by the lack of efficient methods of their characterization. Here we report a robust and efficient method of minor H gene discovery that combines whole genome association scans (WGASs) with cytotoxic T-lymphocyte (CTL) assays, in which the genetic loci of minor H genes recognized by the CTL clones are precisely identified using pooled-DNA analysis of immortalized lymphoblastoid cell lines with/without susceptibility to those CTLs. Using this method, we have successfully mapped 2 loci: one previously characterized (*HMSD* encoding ACC-6), and one novel. The novel minor H antigen encoded by *BCL2A1* was identified within a 26 kb linkage disequilibrium block on chromosome 15q25, which had been directly mapped by WGAS. The pool size required to identify these regions was no more than 100 individuals. Thus, once CTL clones are generated, this method should substantially facilitate discovery of minor H antigens applicable to targeted allo-immune therapies and also contribute to our understanding of human allo-immunity. (Blood. 2008;111: 3286-3294)

Introduction

Currently, allogeneic hematopoietic stem cell transplantation (allo-HSCT) has been established as one of the most effective therapeutic options for hematopoietic malignancies[1] and is also implicated as a promising approach for some solid cancers.[2] Its major therapeutic benefits are obtained from allo-immunity directed against patients' tumor cells (graft-versus-tumor [GVT] effects). However, the same kind of allo-immune reactions can also be directed against normal host tissues resulting in graft-versus-host disease (GVHD). In HLA-matched transplants, both GVT and GVHD are initiated by the recognition of HLA-bound polymorphic peptides, or minor histocompatibility (H) antigens, by donor T cells. Minor H antigens are typically encoded by dichotomous single nucleotide polymorphism (SNP) alleles, and may potentially be targeted by allo-immune reactions if the donor and recipient are mismatched at the minor H loci. Identification and characterization of minor H antigens that are specifically expressed in hematopoietic tissues, but not in other normal tissues, could contribute to the development of selective antileukemic therapies while minimizing unfavorable GVHD reactions, one of the most serious complications of allo-HSCT.[3,4] Unfortunately, the total number of such useful minor H antigens that are currently molecularly characterized is still disappointingly small, including HA-1,[5] HA-2,[6] ACC-1[Y] and ACC-2,[7] DRN-7,[8] ACC-6,[9] LB-ADIR-1F,[10] HB-1,[11] LRH-1,[12] and 7A7-PANE1,[13] limiting the number of patients eligible for such GVT-oriented immunotherapy.

Several techniques have been developed to identify novel minor H antigens targeted by CTLs generated from patients who have undergone transplantation. Among these, linkage analysis based on the cytotoxicity of the CTL clones against panels of lymphoblastoid cell lines (B-LCLs) from large pedigrees was proposed as a novel genetic approach,[14] and has been successfully applied to identify novel minor H epitopes encoded by the *BCL2A1* and *P2RX5* genes.[7,12] Nevertheless, the technology is still largely limited by its resolution, especially when large segregating families are not available. Linkage analysis using B-LCL panels from the Centre d'Etude du Polymorphisme Humain (CEPH) could only localize minor H loci within a range of 1.64 Mb to 5.5 Mb, which still contained 11 to 46 genes,[7,12,14] thus requiring additional selection procedures to identify the actual minor H genes.

On the other hand, clinically relevant minor H antigens might be associated with common polymorphisms within the human

Submitted October 22, 2007; accepted December 19, 2007. Prepublished online as *Blood* First Edition paper, January 4, 2008; DOI 10.1182/blood-2007-10-118950.

T.K. and Y.N. contributed equally to this work.

The online version of this article contains a data supplement.

The publication costs of this article were defrayed in part by page charge payment. Therefore, and solely to indicate this fact, this article is hereby marked "advertisement" in accordance with 18 USC section 1734.

population, and therefore could be ideal targets of genetic association studies, considering recent advances of large-scale genotyping technologies and the assets of the International HapMap Project.[15,16] In this alternative genetic approach using the extensive linkage disequilibrium (LD) found within the human genome, target loci can be more efficiently localized within relatively small haplotype blocks without depending on limited numbers of recombination events, given the large number of genotyped genetic markers.[17] Moreover, since the presence of a target minor H allele in individual target cells can be determined by ordinary immunologic assays using minor H antigen-specific CTLs, the characterization of minor H antigens should be significantly more straightforward than identifying alleles associated with typical common complex diseases, for which typically weak-to-moderate genetic effects have been assumed.[18]

In this report, we describe a high-performance, cost-effective method for the identification of minor H antigens, in which whole genome association scans (WGASs) are performed based on SNP array analysis of pooled DNA samples constructed from cytotoxicity-positive (CTX^+) and cytotoxicity-negative (CTX^-) B-LCLs as determined by their susceptibility to CTL clones. Based on this method, termed WGA/CTL, we were able to map the previously characterized ACC-6 minor H locus to a 115-kb block containing only 4 genes, including *HMSD*.[9] Moreover, using the same approach, a novel minor H antigen encoded by the *BCL2A1* gene was identified within a 26-kb block containing only *BCL2A1* on chromosome 15q25. Surprisingly, the pool size required to identify these regions was no more than 100 individuals. Thus, this WGA/CTL method has significant potential to accelerate the discovery of minor H antigens that could be used in more selective, and thus more effective, allo-immune therapies in the near future.

Methods

Cell isolation and cell cultures

This study was approved by the institutional review board of the Aichi Cancer Center and the University of Tokyo. All blood or tissue samples were collected after written informed consent was obtained in accordance with the Declaration of Helsinki. B-LCLs were derived from allo-HSCT donors, recipients, and healthy volunteers. B-LCLs were maintained in RPMI 1640 medium supplemented with 10% fetal calf serum, 2 mM L-glutamine, 1 mM sodium pyruvate.

Generation of CTL lines and clones

CTL lines were generated from peripheral blood mononuclear cells (PBMCs) obtained after transplantation by stimulation with irradiated (33 Gy) recipient PBMCs harvested before HSCT, thereafter stimulated weekly in RPMI 1640 supplemented with 10% pooled human serum and 2 mM L-glutamine. IL-2 was added on days 1 and 5 after the second and third stimulations. CTL clones were isolated by standard limiting dilution and expanded as previously described.[7] CTL-1B9 was isolated from PBMCs harvested on day 30 after transplantation from a patient receiving a marrow graft from his HLA-identical sibling (HLA A11, A24, B39, B51, Cw7, Cw14), and CTL-2A12 has been described recently.[9]

Chromium release assay

Target cells were labeled with 0.1 mCi (3.7 MBq) of ^{51}Cr for 2 hours, and 10^3 target cells/well were mixed with CTL at the effector-to-target (E/T) ratio indicated in a standard 4-hour cytotoxicity. All assays were performed at least in duplicate. Percent specific lysis was calculated as follows: ((Experimental cpm − Spontaneous cpm) / (Maximum cpm − Spontaneous cpm)) × 100.

Immunophenotyping by enzyme-linked immunosorbent assay

B-LCL cells (20 000 per well, which had been retrovirally transduced with restriction HLA cDNA for individual CTLs, if necessary) were plated in each well of 96-well round-bottomed plates, and corresponding CTL clones (10 000 per well) were added to each well. After overnight incubation at 37°C, 50 μL supernatant was collected and released IFN-γ was measured by standard enzyme-linked immunosorbent assay (ELISA).

Construction of pooled DNA and microarray experiments

Genomic DNA was individually extracted from immunophenotyped B-LCLs. After DNA concentrations were measured and adjusted to 50 μg/mL using the PicoGreen dsDNA Quantitation Reagent (Molecular Probes, Eugene, OR), the DNA specimens from CTX^+ and CTX^- B-LCLs were separately combined to generate individual pools. DNA pools were analyzed in pairs using Affymetrix GeneChip SNP-genotyping microarrays (Affymetrix, Tokyo, Japan) according to the manufacturer's protocol,[19,20] where 2 independent experiments were performed for each array type (for more detailed statistical analysis for generated microarray data, see Document S1, available on the *Blood* website; see the Supplemental Materials link at the top of the online article).

Estimation of LD blocks

LD structures of the candidate loci were evaluated based on empirical data from the International Hap Map Project (http://www.hapmap.org/).[15] LD data for the relevant HapMap panels were downloaded from the HapMap web site and further analyzed using Haploview software (http://www.broad.mit.edu/mpg/haploview/).[21]

Transfection of 293T cells and ELISA

Twenty thousand 293T cells retrovirally transduced with HLA-A*2402 were plated in each well of 96-well flat-bottomed plates, cultured overnight at 37°C, then transfected with 0.12 μg of plasmid containing full-length *BCL2A1* cDNA generated from either the patient or his donor using Trans IT-293 (Mirus, Madison, WI). B-LCLs of the recipient and his donor were used as positive and negative controls, respectively. Ten thousand CTL-1B9 cells were added to each well 20 hours after transfection. After overnight incubation at 37°C, 50 μL of supernatant was collected and IFN-γ was measured by ELISA.

SNP identification by direct sequencing

Complementary DNA prepared from B-LCLs was polymerase chain reaction (PCR) amplified for the coding region of *BCL2A1* using the following primers: sense: 5′-AGAAGATGACAGACTGTGAATTTGG -3′; antisense: 5′-TCAACAGTATTGCTTCAGGAGAG-3′.

PCR products were purified and directly sequenced with the same primer and BigDye Terminator kit (version 3.1) by using ABI PRISM 3100 (Applied Biosystems, Foster City, CA).

Confirmatory SNP genotyping

Genotyping was carried out using fluorogenic 3′-minor groove binding (MGB) probes in a PCR assay. PCR was conducted in 10-μL reactions containing both allelic probes, 500 nM each of the primers, 1 × TaqMan Universal PCR Master Mix (Applied Biosystems), and 1 μL (100 ng) DNA. PCR cycling conditions were as follows: predenature, 50°C for 2 minutes, 95°C for 10 minutes, followed by 35 cycles of 92°C for 15 seconds and 60°C for 1 minute in a GeneAmp PCR System 9700 (Applied Biosystems). The PCR products were analyzed on an ABI 7900HT with the aid of SDS 2.2 software (Applied Biosystems).

Epitope reconstitution assay

The candidate *BCL2A1*-encoded minor H epitope and its allelic counterpart (DYLQYVLQI) peptides were synthesized by standard Fmoc chemistry. ^{51}Cr-labeled CTX^- donor B-LCLs were incubated with graded concentrations of the peptides and then used as targets in standard cytotoxicity assays.

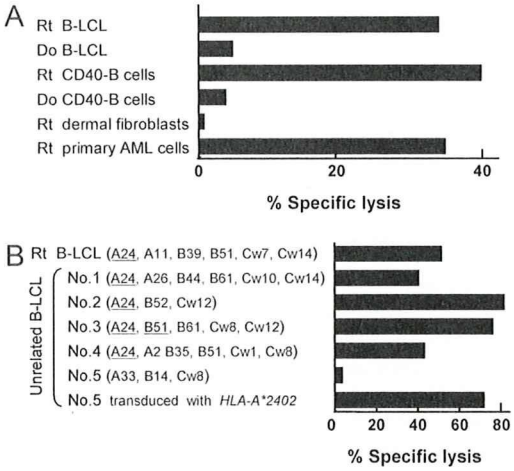

Figure 1. Specificity of CTL-1B9 against hematopoietic cells and its restriction HLA. (A) The cytolytic activity of CTL-1B9 was evaluated in a standard 4-hour ^{51}Cr release assay (E/T ratio, 20:1). Targets used were B-LCL, CD40-activated (CD40-B) B cells, dermal fibroblasts, and primary acute myeloid leukemia cells from the recipient (Rt), and B-LCL and CD40-B cells from his donor (Do). Rt dermal fibroblasts were pretreated with 500 U/mL IFN-γ and 10 ng/mL TNF-α for 48 hours before ^{51}Cr labeling. (B) Cytolytic activity of CTL-1B9 against a panel of B-LCLs derived from unrelated individuals, each of whom shared 1 or 2 class I MHC allele(s) with the recipient from whom the CTL-1B9 was generated. The shared HLA allele(s) with the recipient are underlined. B-LCLs (no. 5) which did not share any HLA alleles with the recipient, were retrovirally transduced with HLA-A*2402 cDNA and included to confirm HLA-A*2402 restriction by CTL-1B9. Results are typical of 2 experiments and data are the mean plus or minus the standard deviation (SD) of triplicates.

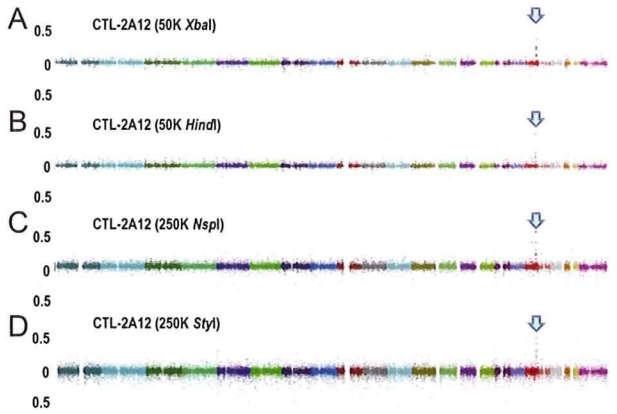

Figure 2. Whole genome association scans performed with pooled DNA generated based on immunophenotyping with CTL-2A12. Pooled DNAs generated from 44 CTX$^+$ and 44 CTX$^-$ B-LCLs were analyzed with 50 K *Xba*I (A), 50 K *Hin*dIII (B), 250 K *Nsp*I (C), and 250 K *Sty*I (D) arrays. Test statistics were calculated for all SNPs and plotted in the chromosomal order. In all SNP array types, a common association peak is observed at 18q21, to which the minor H antigen for CTL-2A12, encoded by the *HMSD* gene, had been mapped based on expression cloning[9] (arrows).

Results

CTL-based typing and SNP array analysis of pooled DNA

CTL-2A12 and CTL-1B9 are CTL clones established from the peripheral blood of 2 patients with leukemia who had received HLA-identical sibling HSCTs. Each clone demonstrated specific lysis against the B-LCLs of the recipient but not against donor B-LCLs, indicating recognition of minor H antigen (Figure 1A and Kawase et al[9]). The minor H antigen for CTL-2A12 had been previously identified by expression cloning[9]; on the other hand, the target minor H antigen for the HLA-A24–restricted CTL-1B9 clone, which was apparently hematopoietic lineage–specific (Figure 1A) and present in approximately 80% of the Japanese population (data not shown), had not yet been determined. Using these CTL clones, a panel of B-LCLs expressing the restriction HLA (HLA-B44 for CTL-2A12 and HLA-A24 for CTL-1B9) endogenously or retrovirally transduced, were subjected to "immunophenotyping" for the presence or absence of the minor H antigen by ELISA and, if necessary, by standard chromium release assay (CRA). Based on the assay results, for CTL-2A12 we initially collected 44 cytotoxicity-positive (CTX$^+$) and 44 cytotoxicity-negative (CTX$^-$) B-LCLs after screening 132 B-LCLs, while 57 CTX$^+$ and 38 CTX$^-$ B-LCLs were obtained from 121 B-LCLs for CTL-1B9. From these sets of B-LCL panels, pools of DNA were generated and subjected to analysis on Affymetrix GeneChip 100 K and 500 K microarrays in duplicate.[19,20]

Detection of association between minor H phenotypes and marker SNPs

Genetic mapping of the minor H locus was performed by identifying marker SNPs that showed statistically significant deviations in allele-frequencies between CTX$^+$ and CTX$^-$ pools based on the observed allele-specific signals in the microarray experiments. For this purpose, we evaluated the deviations of observed allele ratios between CTX$^+$ and CTX$^-$ pools for each SNP on a given array (Document S1). An SNP was considered as positive for association if its test statistic exceeded an empirically determined threshold that provided a "genome-wide" P value of .05 in duplicate experiments (Document S1, Figures S1,S2, and Table S1). Threshold values for different pool sizes are also provided in Table S2 for further experiments. The positive SNPs eventually obtained for both CTLs are summarized in Table 1, where the 10 SNPs showing the highest test statistics are listed for individual experiments.

Mapping of the minor H loci by WGASs

All the SNPs significantly associated with susceptibility to CTL-2A12 were correctly mapped within a single 115 kb LD block at chromosome 18q21 containing the *HMSD* gene (Figures 2 and 3A), which had been previously shown to encode the ACC-6 minor H antigen recognized by CTL-2A12.[9] According to the above criteria, no false-positive SNPs were reported in any array types (Table 1). Confirmation genotyping of individual B-LCLs from both panels revealed none of the 44 that had been immunophenotyped as CTX$^-$ were misjudged, while 8 of the 44 CTX$^+$ B-LCLs were found to actually carry no minor H-positive allele for ACC-6, which was likely due to the inclusion of individual B-LCLs showing borderline cytotoxicity (data not shown).

On the other hand, positive association of the target minor H antigen with CTL-1B9 was detected in 2 independent loci: SNP rs1879894 at 15q25.1 in 250 K *Nsp*I (Table 1, Figure 4A-B, and Figure S5) and SNP rs1842353 at 8q12.3 in 50 K *Hin*dIII (Table 1 and Figure S3A). We eventually focused on rs1879894, as it showed a much more significant genome-wide P value than SNP rs1842353 (Table 1). In contrast to the CTL-2A12 case, where many mutually correlated SNPs around the most significant one created a broad peak in the statistic plots (Figure 2 arrows and Figure S3), the adjacent SNPs (rs6495463 and rs2562756; Figure 3B solid arrows) around rs187894 (Figure 3B open arrow) did not show large test statistic values, reflecting the fact that no marker SNPs on 100 K and 500 K arrays exist in high LD (Figure 3B dashed red lines encompassing 26 kb) with this SNP according to the HapMap data. To further confirm the association, we generated additional B-LCL pools consisting of 75 CTX$^+$ and 34 CTX$^-$

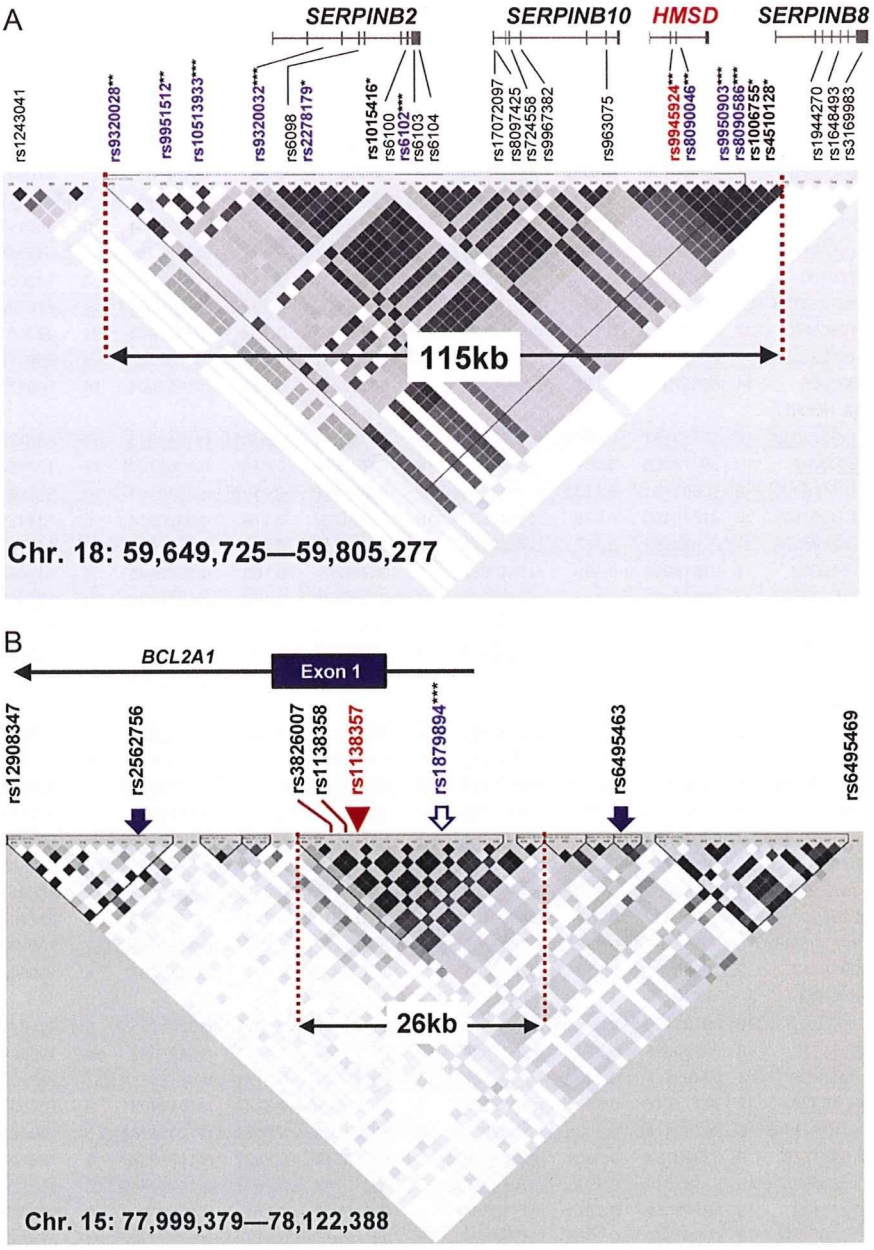

Figure 3. Linkage disequilibrium (LD) block mapped by CTL-2A12 and CTL-1B9. (A) An LD block map identified by pairwise r^2 plot from HapMap CEU data are overlayed with SNPs available from Affymetrix GeneChip SNP-genotyping microarrays (arrows) and 4 genes in the 115 kb block. SNPs that emerged repeatedly in the 2 independent experiments are indicated in blue. The genomewide *P* values for positive SNPs are shown as follows: $*P < .05$; $**P < .01$; $***P < .001$. The intronic SNP (rs9945924) controlling the alternative splicing of *HMSD* transcripts and expression of encoded ACC-6 minor H antigen is indicated in red. (B) LD blocks identified by pairwise r^2 plot from HapMap JPT data are overlayed with SNPs available from Affymetrix GeneChip SNP-genotyping microarrays (arrows) and exon 1 of the *BCL2A1* gene. The only SNP showing a high association with CTL-1B9 immunophenotypes (rs1879894) is shown as an open arrow. The nonsynonymous SNP (rs1138357) controlling the expression of the minor H antigen recognized by CTL-1B9 is indicated by a red arrowhead. ***SNP with genomewide $P < .001$. The 2 SNPs adjacent to the 26 kb LD block (rs2562756 and rs6495463) never gave a significant genomewide *P* value.

B-LCLs from another set of 128 B-LCLs, and performed a WGAS. As expected, the WGAS of the second pools also identified the identical SNP with the highest test statistic value in duplicate experiments, unequivocally indicating that this SNP is truly associated with the minor H locus of interest (Figure 4C,D and Table S3). The association was also detected when the references in the first and second pools were swapped (data not shown).

Identification of the minor H epitope recognized by CTL-1B9

The LD block containing SNP rs1879894 that was singled out from more than 500 000 SNP markers with 2 sets of DNA pools only encodes exon 1 of *BCL2A1* (Figure 3B). To our surprise, this was the region to which we had previously mapped an HLA-A24–restricted minor H antigen, ACC-1^Y.[7] We first confirmed that full-length *BCL2A1* cDNA cloned only from the recipient but not his donor could stimulate interferon-γ secretion from CTL-1B9 when transduced into donor B-LCL (Figure 5A), indicating that *BCL2A1* is a bona fide gene encoding minor H antigen recognized by CTL-1B9. We next genotyped 3 nonsynonymous SNPs in the *BCL2A1* exon 1 sequence (Figure 3B) and comparison was made between the genotypes and the susceptibility to CTL-1B9 of 9 HLA-A*2402$^+$ B-LCLs, including ones generated from the recipient (from whom CTL-1B9 was established) and his donor. Susceptibility to CTL-1B9 correlated completely with the presence of guanine at SNP rs1138357 (nucleotide position 238, according to the mRNA sequence for NM_004049.2) and thymine at SNP rs1138358 (nucleotide position 299) (Table 2), suggesting that the expression of the minor H epitope recognized by CTL-1B9 is controlled by either of these SNPs. We searched for nonameric amino acid sequences spanning the 2 SNPs using BIMAS software,[22] since most reported HLA-A*2402 binding peptides contain 9 amino acid residues.[23] Among these, a nonameric peptide, DYLQ*C*VLQI (the polymorphic residue being underlined), has a predicted binding score of 75 and was considered as a candidate minor H epitope. As shown in Figure 5B, the DYLQ*C*VLQI was strongly recognized by CTL-1B9, whereas its allelic counterpart,

Table 1. Positive SNPs from pooled DNA analysis

CTL-2A12, Exp 1				CTL-2A12, Exp 2				CTL-1B9, Exp 1				CTL-1B9, Exp 2			
rsID	Chr	Position	$\Delta R_{A\Delta R_B}$	rsID	Chr	Position	$\Delta R_{A\Delta R_B}$	rsID	Chr	Position	$\Delta R_{A\Delta R_B}$	rsID	Chr	Position	$\Delta R_{A\Delta R_B}$
50K X bal															
rs10513933	18	59699669	0.366*	rs10513933	18	59699669	0.511†	rs1363258	5	103297593	0.239	rs10499174	6	131209689	0.352*
rs9320028	18	59668150	0.255‡	rs9320028	18	59668150	0.360*	rs726083	3	67093729	0.203	rs30058	5	122325602	0.240
rs6102	18	59721450	0.221	rs10485873	7	3503743	0.157	rs639243	5	31392931	0.198	rs150724	16	61960443	0.213
rs724533	23	116440574	0.137	rs219323	14	59510440	0.150	rs1936461	10	56519024	0.186	rs1993129	8	63618836	0.208
rs1341112	6	104919391	0.136	rs10506892	12	82478539	0.147	rs763876	12	94922502	0.186	rs356946	13	69066751	0.201
rs470490	18	61182216	0.136	rs10492269	12	97786333	0.144	rs958404	7	133054441	0.179	rs2869268	4	86421898	0.184
rs2826718	21	21471423	0.134	rs10483466	14	35986827	0.139	rs10486727	7	41672315	0.178	rs287002	12	40312537	0.183
rs10506697	12	73241741	0.128	rs5910124	23	116408616	0.137	rs2833488	21	32010112	0.176	rs1146808	13	67688608	0.182
rs10506891	12	82393029	0.127	rs10512545	17	66337079	0.134	rs379212	5	60977687	0.172	rs10501287	11	42446011	0.180
rs308995	14	59657919	0.125	rs295678	5	58186928	0.131	rs1954004	14	58627872	0.170	rs564993	5	31393476	0.177
50K *Hind*III															
rs9320032	18	59712191	0.486†	rs9320032	18	59712191	0.506†	rs1842353	8	63617543	0.244*	rs9300692	13	101216476	0.225‡
rs8090046	18	59773066	0.207‡	rs8090046	18	59773066	0.245*	rs10521202	17	12755289	0.201‡	rs1842353	8	63617543	0.210‡
rs1474220	2	108525317	0.193‡	rs10498752	6	41876488	0.210‡	rs7899961	10	59696431	0.198‡	rs10520983	5	31314700	0.195‡
rs10498752	6	41876488	0.178	rs1941538	18	37994337	0.176	rs9320974	6	124421441	0.197‡	rs1334375	13	80897038	0.173
rs2298578	21	21632551	0.167	rs7682770	4	152748018	0.174	rs10520983	5	31314700	0.179	rs10519164	15	75412758	0.163
rs7516032	1	91618962	0.165	rs1445862	5	3675257	0.169	rs1862446	5	147460749	0.170	rs9322063	6	146852196	0.152
rs5030938	10	70645922	0.164	rs4696976	4	21058616	0.167	rs1358778	20	13266796	0.169	rs8067384	17	37926265	0.150
rs1883041	21	44921845	0.158	rs5030938	10	70645922	0.165	rs1873790	4	83422480	0.166	rs10521202	17	12755289	0.147
rs3902916	4	189045176	0.155	rs3902916	4	189045176	0.165	rs1220724	4	70888705	0.162	rs7914904	10	62749969	0.141
rs1000551	20	58709208	0.154	rs1883041	21	44921845	0.164	rs9300692	13	101216476	0.157	rs1220724	4	70888705	0.141
250K *Nsp*I															
rs9950903	18	59781783	0.534†	rs9950903	18	59781783	1.036†	rs1879894	15	78055874	0.846†	rs1879894	15	78055874	1.072†
rs1463835	3	23539615	0.532†	rs8090586	18	59781864	0.518†	rs9646294	16	6110019	0.484†	rs6771859	3	190642054	0.387†
rs16975459	18	37802275	0.383*	rs6473170	8	80664840	0.338*	rs17734332	5	134945240	0.365†	rs10512261	9	98804394	0.299*
rs8090586	18	59781864	0.367*	rs4510128	18	59782312	0.310‡	rs566619	7	41381538	0.345*	rs12122772	1	60384564	0.287*
rs16872621	4	22081055	0.312‡	rs1006755	18	59782026	0.300‡	rs17737566	6	50345280	0.310*	rs2153155	4	26034162	0.248‡
rs870582	6	125097114	0.301‡	rs7039378	9	118735938	0.258	rs3849955	9	28350374	0.285*	rs17126896	14	53320494	0.246‡
rs1015416	18	59720363	0.270‡	rs1860563	16	6418899	0.258	rs4616156	13	86581518	0.273*	rs1328652	13	35607527	0.240
rs2155907	11	97599883	0.227	rs4699126	4	105709109	0.212	rs2484698	1	217474460	0.263*	rs7021551	9	27446645	0.237
rs2112948	5	50994294	0.222	rs10275055	7	156212079	0.204	rs17139603	11	79638632	0.262*	rs252817	5	106752487	0.237
rs2919747	2	129681506	0.217	rs1526411	7	124658309	0.201	rs2156737	4	100642529	0.246‡	rs10772587	12	12681356	0.235
250K *Sty*I															
rs6102	18	59721450	0.597†	rs6102	18	59721450	0.495†	rs9383925	6	151975774	0.819†	rs201204	6	104842863	0.688†
rs9951512	18	59690885	0.374*	rs9945924	18	59771746	0.407*	rs6497397	16	19646258	0.311‡	rs12556155	23	108836419	0.442†
rs6496897	15	90493249	0.320‡	rs9951512	18	59690885	0.317‡	rs917252	7	22219990	0.289‡	rs4791422	17	10605304	0.435†
rs9945924	18	59771746	0.315‡	rs1983205	3	157782892	0.314‡	rs1019403	3	7823997	0.260‡	rs7749012	6	106459559	0.336*
rs12707805	8	107404746	0.303‡	rs950865	5	2720684	0.307‡	rs17053134	5	155373544	0.259‡	rs509951	5	31385483	0.308‡
rs10971778	9	33893184	0.296‡	rs2278179	18	59715512	0.292‡	rs11710880	3	72214965	0.246	rs16879024	8	32225711	0.256‡
rs6565076	16	81487818	0.294‡	rs10427722	22	36417752	0.289‡	rs17167866	7	13919264	0.237	rs2100054	15	75293482	0.252
rs2278179	18	59715512	0.291‡	rs17156659	7	82046820	0.271	rs10867062	9	137935241	0.237	rs11811023	1	143805934	0.240
rs7806238	7	29906442	0.290‡	rs4502324	18	4811261	0.262	rs5925800	23	23278707	0.235	rs17382798	15	75256074	0.231
rs965888	18	38062658	0.283‡	rs1348428	2	225927288	0.260	rs2255831	4	146614313	0.234	rs2030302	17	12526591	0.231

Significant SNPs that appeared on both experiments are underlined.
*Genomewide $P < .01$.
†Genomewide $P < .001$.
‡Genomewide $P < .05$.

DYLQ*Y*VLQI, was not. Decameric peptide, QDYLQ*C*VLQI, on the other hand, appeared to be weakly recognized; however, it is likely that the nonameric form was actually being presented after N-terminal glutamine cleavage by aminopeptidase in the culture medium. Because it was possible that the cystine might be cysteinylated, recognition of synthetic peptides DYLQCVLQI and cysteinylated DYLQC*VLQI were assayed using CTL-1B9. Half-maximal lysis for the former was obtained at a concentration of 200 pM, whereas recognition of the latter was several-fold weaker (Figure 5C). Thus, we concluded that DYLQCVLQI defines the cognate HLA-A*2402–restricted CTL-1B9 epitope, now designated ACC-1^C. This incidentally provides a second example of products from both dichotomous SNP alleles being recognized as HLA-A*2402–restricted minor H antigens, the first example being the HB-1 minor H antigen.[24] Finally, real-time quantitative PCR revealed that T cells carrying the complementarity-determining region 3 sequence identical to CTL-1B9 became detectable in the patient's blood at the frequencies of 0.22%, 0.91%, 1.07% and 0.01% among $TCR\alpha\beta^+$ T cells at days 30, 102, 196, and 395 after transplantation, respectively, suggesting that ACC-1^C minor H antigen is indeed immunogenic (Figure 5D).

Discussion

Recent reports have unequivocally demonstrated that WGASs can be successfully used to identify common variants involved in a wide variety of human diseases.[25-27] Our report represents a novel

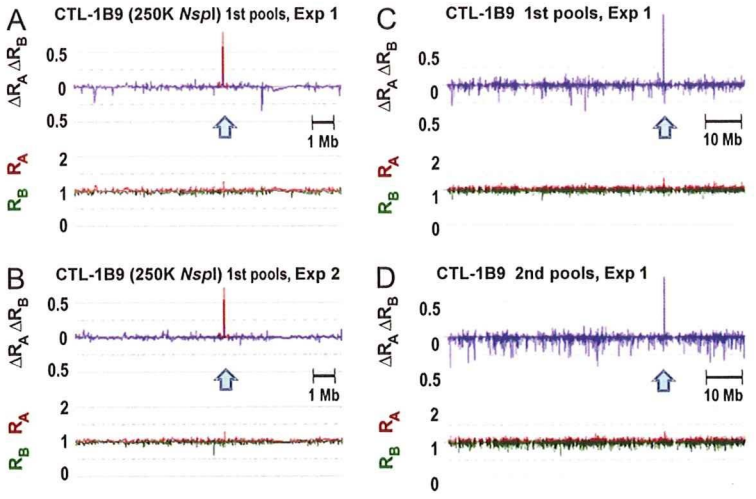

Figure 4. Reproducible detection of association with the immunophenotypes determined by CTL-1B9 at the *BCL2A1* locus. The maximum test statistic value was observed at a single SNP (rs1879894) within 15q25.1 in duplicate experiments for the first pools consisting of 57 CTX^+ and 38 CTX^- B-LCLs (A-C). The peak association at the same SNP was reproduced in the experiments with the second pools consisting of 75 CTX^+ and 34 CTX^- LCLs (D). Test statistic values ($\Delta R_A \Delta R_B$) are plotted by blue lines together with their R_A (red) and R_B (green) values. The expected $\Delta R_A \Delta R_B$ values multiplied by r^2 correlation coefficients for the adjacent SNPs within 500 kb from the SNP rs1879894 are overlaid by red lines (A,B).

application of WGASs to transplantation immunology, which provides a simple but robust method to fine-map the genetic loci of minor H antigens whose expression is readily determined by standard immunophenotyping with CTL clones established from patients who have undergone transplantation.

The current WGA/CTL method has several desirable features that should contribute to the acceleration of minor H locus mapping. In comparing the method to those of linkage analysis and other nongenetic approaches, including direct peptide sequencing of chemically purified minor H antigens[5,6,10,13] and conventional

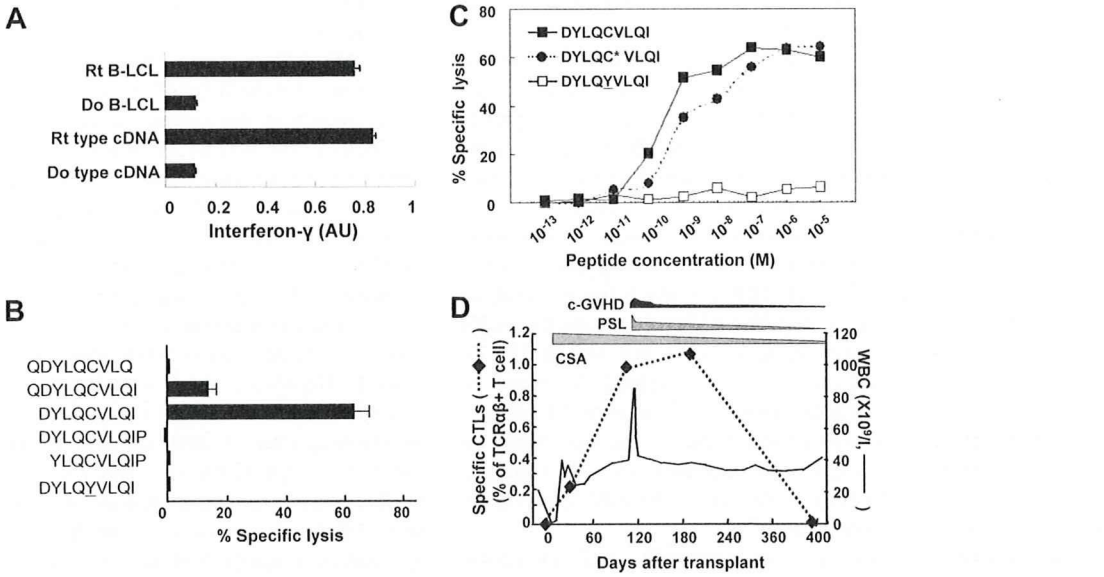

Figure 5. Identification of the CTL-1B9 minimal minor H epitope. (A) Interferon-γ production from CTL-1B9 against HLA-A*2402–transduced 293T cells transfected with plasmid encoding full-length *BCL2A1* cDNA cloned from either the recipient (Rt) from whom CTL-1B9 was isolated or his donor (Do). Rt B-LCL and Do B-LCL were used as positive and negative controls, respectively. Secreted interferon-γ was measured by ELISA and is expressed in arbitrary units (AUs) corresponding to optical density at 630 nm. Results are typical of 2 experiments and data are the mean plus or minus SD of triplicates. (B) A peptide reconstitution assay was conducted to determine the minimal epitope for CTL-1B9. Nonameric peptide (DYLQCVLQI), 2 nonameric peptides shifted by one amino acid to N- or C-terminus, N- and C-terminal extended decameric peptides, and its allelic counterpart (DYLQ**Y**VLQI) were synthesized and tested by adding to antigen-negative donor B-LCL at 10 nM in a standard ^{51}Cr release assay. Results are typical of 2 experiments and data are the mean plus or minus SD of triplicates. (C) Titration of the candidate minor H peptide by epitope reconstitution assay. Chromium-labeled donor B-LCLs were distributed to wells of 96-well round-bottomed plates, pulsed with serial dilutions of the indicated peptides for 30 minutes at room temperature, and then used as targets for CTL-1B9 in a standard ^{51}Cr release assay. A cysteinylated peptide (indicated by an asterisk) was included as an alternative form of the potential epitope. Results are typical of 2 experiments. (D) Tracking of ACC-1^C–specific T cells in the recipient's peripheral blood. In order to longitudinally analyze the kinetics of the ACC-1^C–specific CTLs in peripheral blood from the patient from whom CTL-1B9 was established, a real-time quantitative PCR was conducted. Complementary DNAs of peripheral blood mononuclear cells from the donor and patient before and after HSCT were prepared from the patient. Real-time PCR analysis was performed using a TaqMan assay as described previously.[9] The primers and fluorogenic probe sequences spanning the CTL-1B9 complementarity-determining region 3 (CDR3) were used to detect T cells carrying the CDR3 sequences identical to that of CTL-1B9. The primers and fluorogenic probe sequences spanning constant region of TCR beta chain (TCRBC) mRNA were used as internal control. Samples were quantified with the comparative CT method. The delta CT value was determined by subtracting the average CT value for TCRBC from the average CTL-1B9 CDR3 CT value. The standard curve for the proportion of CTL-1B9 among $TCR\alpha\beta^+$ T cells was composed by plotting mean delta CT values for each ratio, and the percentages of T cells carrying the CDR3 sequence identical to CTL-1B9 were calculated by using this standard curve. During this period, quiescent chronic GVHD, which required steroid treatment, developed; however, involvement of immune reaction to ACC-1^C minor H antigen was unlikely since its frequency increased even after resolution of most chronic GVHD symptoms. c-GVHD, chronic GVHD; CSA, cyclosporine A; PSL, prednisolone; WBC, white blood cell count.

Table 2. Correlation of *BCL2A1* sequence polymorphisms with susceptibility to CTL-1B9

	HLA-A*2402–positive B-LCLs								
	Rt	Do	UR1	UR2	UR3	UR4	UR5	UR6	UR7
Cytolysis by CTL-1B9	+	−	+	+	+	+	+	−	−
Detected SNP, position*									
rs1138357, 238	G/A	A	G	G	G/A	G/A	G/A	A	A
rs1138358, 299	T/G	G	T	T	T/G	T/G	T/G	G	G
rs3826007, 427	G	G/A	G	G	G	G	G/A	G/A	G

Rt indicates recipient; Do, donor; UR, unrelated; +, yes; and −, no.

*Nucleotide positions are shown according to the NM_004092.2 mRNA sequence, available at http://www.ncbi.nlm.nih.gov/ as GEO accession GSE10044.

expression cloning,[8,9,11] there are differences in terms of power, sensitivity, and specificity. Direct sequencing of minor H antigen peptide guarantees that the purified peptide is surely present on the cell surface as antigen, but it requires highly specialized equipment and personnel. Expression screening of cDNA libraries is also widely used and has become feasible with commercially available systems. However, it depends highly on the quality of the cDNA library and expression levels of the target genes. In addition, it often suffers from false-positive results due to the forced expression of cDNA clones under a strong promoter. The current method of WGA/CTL genetically determines the relevant minor H antigen locus, not relying on highly technical protein chemistry using specialized equipment, or repetitive cell cloning procedures. It is also not affected by the expression levels of the target antigens.

As a genetic approach, the current method based on genetic association has several advantages over conventional linkage analysis: the mapping resolution has been greatly improved from several Mb in the conventional linkage analysis to the average haplotype block size of less than 100 kb,[17,25-27] usually containing a handful of candidate genes, compared with the dozens as typically found in linkage analysis. This means that the effort needed for the subsequent epitope mapping will be substantially reduced. In fact, the 115 kb region identified for CTL-2A12 contains 4 genes compared with 38 genes as revealed by the previous linkage study (data not shown), and the candidate gene was uniquely identified within the 26 kb region for CTL-1B9, for which linkage analysis had failed due to very rare segregating pedigrees among the CEPH panels with this trait (now ACC-1[C]; data not shown).[15,16] In addition, before moving on to epitope mapping, it would be possible to evaluate the clinical relevance of the minor H antigens by examining the tissue distribution of their expression, based on widely available gene expression databases such as Genomic Institute of the Novartis Research Foundation (GNF, http://symatlas.gnf.org/SymAtlas/).[28]

Second, the required sample size is generally small, and should be typically no more than 100 B-LCLs for common minor H alleles. This is in marked contrast to the association studies for common diseases, in which frequently thousands of samples are required.[17,25-27] In the current approach, sufficiently high test statistic values could be obtained for the relevant loci with a relatively small sample size, since the minor H allele is correctly segregated between the CTX^+ and CTX^- pools by the highly specific immunologic assay. Combined with high accuracy in allelic measurements, this feature allows for the use of pooled DNAs in WGAS, which substantially saves cost and time, compared with the genotyping of individual samples. Unexpectedly, our method allows for a considerable degree of error in the immunophenotyping, indicating the robustness of the current method; in fact, the minor H locus for CTL-2A12 was successfully identified in spite of the presence of 8 (~10%) immunophenotyping errors. When the minor H allele has an extreme allele frequency (eg, $< 5\%$ or $> 95\%$), which could be predicted by preliminary immunophenotyping, WGAS/CTL may not be an efficient method of mapping, due to the impractically large numbers of B-LCLs that would need to be screened to obtain enough CTX^+ or CTX^- B-LCLs. However, such minor H antigens would likely have limited clinical impact or applicability.

Sensitivity of the microarray analysis seems to be very high when the target SNP has good proxy SNPs on the array, because we were able to correctly identify the single SNP correlated with the target of CTL-1B9 from more than 500 000 SNP markers. On the other hand, genome coverage of the microarray is definitely important. In our experiments on CTL-2A12, the association was successfully identified by the marker SNPs showing r^2 values of approximately 0.74 with the target locus of ACC-6. Since the GeneChip 500 K array set captures approximately 65% of all the HapMap phase II SNPs with more than 0.74 of r^2;[29] and higher coverage will be obtained with the SNP 6.0 arrays having more than 1 000 K SNP markers, these arrays can be satisfactorily used as platforms for the WGA/CTL method.

As shown in the current study, the intrinsic sensitivity and specificity of the WGA/CTL method in detecting associated SNPs were excellent. In other words, as long as target SNPs are captured in high r^2 values with one or more marker SNPs within the Affymetrix 500 K SNP set, there is a high likelihood of capturing the SNP with the current approach. To evaluate the probability of a given minor H antigen being captured in high r^2 with marker SNPs, we checked the maximum r^2 values of known minor H antigen SNPs with the Affymetrix 500 K SNPs, according to empirical data from the HapMap project (www.hapmap.org). Among 13 known minor H antigens, 7 have their entries (designated minor H SNP) in the HapMap phase II SNP set (HA-3,[30] HA-8,[31] HB-1,[11] ACC-1 and ACC-2,[7] LB-ADIR-1F,[10] and 7A7-PANE1[13]), and were used for this purpose (note that absence of their entries in the HapMap data set does not necessarily mean that they could not be captured by a particular marker SNP set). As shown in Table S4, all 7 minor H SNPs are captured by at least one flanking SNP that is included in the Affymetrix 500 K SNP set with r^2 values of more than 0.74 in at least one HapMap panel. The situation should be more favorable in the recently available SNP 6.0 array set with 1 000 K SNPs, indicating the genome coverage with currently available SNP arrays would be sufficient to capture typical minor H antigens with our approach.

Most patients who have received allo-HSCT could be a source of minor H antigen-specific CTL clones to be used for this assay, since the donor T cells are in vivo primed and many CTL clones could be established using currently available methods. In fact, substantial numbers of CTL clones have been established worldwide and could serve as the probes to identify novel minor H antigens.[32,33] Once constructed, a panel of B-LCLs, including those transduced with HLA cDNAs, could be commonly applied to immunophenotyping with different CTL clones, especially when

CTLs are obtained from the same ethnic group. In addition, by adopting other immunophenotyping readouts such as production of IL-2 from $CD4^+$ T cells, this method could be applied to identification of MHC class II–restricted minor H antigens which have crucial roles in controlling CTL functions upstream. This may open a new field in the study of allo-HSCT since MHC class II–restricted mHags have been technically difficult to identify by conventional methods.

Finally, the discovery of ACC-1^C as a novel minor H antigen indicates that all the mismatched transplants at this locus could be eligible for allo-immune therapies, since we have previously demonstrated that the counter allele also encodes a minor H antigen, ACC-1^Y, which is preferentially expressed and presented on blood components including leukemic cells and may serve as a target of allo-immunity.[7,34] Indeed, CTLs specific for ACC-2, an HLA-B44–restricted minor H antigen restricted by the third exonic SNP on *BCL2A1*,[7] was independently isolated from the peripheral blood of a patient with recurrent leukemia re-entering complete remission after donor lymphocyte infusion.[32] The number of eligible allo-HSCT recipients has now been effectively doubled, accounting for 50% of transplants with HLA-A24 or 20% of all transplantations performed in the Asian population. In conclusion, we have described a simple but powerful method for minor H mapping to efficiently accelerate the discovery of novel minor H antigens that will be needed to contribute to our understanding of the molecular mechanism of human allo-immunity.

Acknowledgments

The authors thank Dr W. Ho for critically reading the manuscript; Dr Keitaro Matsuo, Dr Hiroo Saji, Dr Etsuko Maruya, Dr Mamoru Ito, Ms Keiko Nishida, Dr Ayako Demachi-Okamura, Ms Yasuko Ogino, Ms Hiromi Tamaki, and the staff members of the transplant center, donor centers, and the Japan Marrow Donor Program office for their generous cooperation and expert technical assistance.

This study was supported in part by Scientific Research on Priority Areas (B01; no.17016089) from the Ministry of Education, Culture, Science, Sports, and Technology, Japan; Research on Human Genome, Tissue Engineering Food Biotechnology and the Second and Third Team Comprehensive 10-year Strategy for Cancer Control (no. 26), from the Ministry of Health, Labor, and Welfare, Japan; and a Grant-in-Aid from Core Research for Evolutional Science and Technology (CREST) of Japan.

Authorship

Contribution: T.K. performed most immunologic experiments and preparation of pooled DNA and quantative PCR, analyzed data, and wrote the manuscript; Y.N. performed the majority of genetic analyses and analyzed the data; H.T. performed T-cell receptor analysis and designed q-PCR primers and probes; G.Y. contributed to the organization of software for linkage analysis and simulation; S.M. prepared the pooled DNA; M.O., K.M., Y.K, and Y.M. collected clinical data and specimens; T.T. and K.K. contributed to data analysis and interpretation, and to the writing of the article; S.O. and Y.A. supervised the entire project, designed and coordinated most of the experiments in this study, contributed to manuscript preparation, and are senior coauthors.

Conflict-of-interest disclosure: The authors declare no competing financial interests.

Correspondence: Seishi Ogawa, Department of Hematology and Oncology, Department of Regeneration Medicine for Hematopoiesis, The 21st Century COE Program, Graduate School of Medicine, University of Tokyo, 7-3-1, Hongo, Bunkyo-ku, Tokyo 113-8655, Japan; e-mail: sogawa-tky@umin.ac.jp; or Yoshiki Akatsuka, Division of Immunology, Aichi Cancer Center Research Institute, 1-1 Kanokoden, Chikusa-ku, Nagoya 464-8681, Japan; e-mail: yakatsuk@aichi-cc.jp.

References

1. Thomas ED Sr. Stem cell transplantation: past, present and future. Stem Cells. 1994;12:539-544.
2. Childs RW, Barrett J. Nonmyeloablative allogeneic immunotherapy for solid tumors. Annu Rev Med. 2004;55:459-475.
3. Goulmy E. Human minor histocompatibility antigens: new concepts for marrow transplantation and adoptive immunotherapy. Immunol Rev. 1997;157:125-140.
4. Bleakley M, Riddell SR. Molecules and mechanisms of the graft-versus-leukaemia effect. Nat Rev Cancer. 2004;4:371-380.
5. den Haan JM, Meadows LM, Wang W, et al. The minor histocompatibility antigen HA-1: a diallelic gene with a single amino acid polymorphism. Science. 1998;279:1054-1057.
6. Pierce RA, Field ED, Mutis T, et al. The HA-2 minor histocompatibility antigen is derived from a diallelic gene encoding a novel human class I myosin protein. J Immunol. 2001;167:3223-3230.
7. Akatsuka Y, Nishida T, Kondo E, et al. Identification of a polymorphic gene, BCL2A1, encoding two novel hematopoietic lineage-specific minor histocompatibility antigens. J Exp Med. 2003;197:1489-1500.
8. Warren EH, Vigneron NJ, Gavin MA, et al. An antigen produced by splicing of noncontiguous peptides in the reverse order. Science. 2006;313:1444-1447.
9. Kawase T, Akatsuka Y, Torikai H, et al. Alternative splicing due to an intronic SNP in HMSD generates a novel minor histocompatibility antigen. Blood. 2007;110:055-1063.
10. van Bergen CA, Kester MG, Jedema I, et al. Multiple myeloma-reactive T cells recognize an activation-induced minor histocompatibility antigen encoded by the ATP-dependent interferon-responsive (ADIR) gene. Blood. 2007;109:4089-4096.
11. Dolstra H, Fredrix H, Maas F, et al. A human minor histocompatibility antigen specific for B cell acute lymphoblastic leukemia. J Exp Med. 1999;189:301-308.
12. de Rijke B, van Horssen-Zoetbrood A, Beekman JM, et al. A frameshift polymorphism in P2X5 elicits an allogeneic cytotoxic T lymphocyte response associated with remission of chronic myeloid leukemia. J Clin Invest. 2005;115:3506-3516.
13. Brickner AG, Evans AM, Mito JK, et al. The PANE1 gene encodes a novel human minor histocompatibility antigen that is selectively expressed in B-lymphoid cells and B-CLL. Blood. 2006;107:3779-3786.
14. Warren EH, Otterud BE, Linterman RW, et al. Feasibility of using genetic linkage analysis to identify the genes encoding T cell-defined minor histocompatibility antigens. Tissue Antigens. 2002;59:293-303.
15. Consortium TIH. The International HapMap Project. Nature. 2003;426:789-796.
16. Consortium TIH. A haplotype map of the human genome. Nature. 2005;437:1299-1320.
17. Risch N, Merikangas K. The future of genetic studies of complex human diseases. Science. 1996;273:1516-1517.
18. Hirschhorn JN, Daly MJ. Genome-wide association studies for common diseases and complex traits. Nat Rev Genet. 2005;6:95-108.
19. Kennedy GC, Matsuzaki H, Dong S, et al. Large-scale genotyping of complex DNA. Nat Biotechnol. 2003;21:1233-1237.
20. Matsuzaki H, Dong S, Loi H, et al. Genotyping over 100 000 SNPs on a pair of oligonucleotide arrays. Nat Methods. 2004;1:109-111.
21. Barrett JC, Fry B, Maller J, Daly MJ. Haploview: analysis and visualization of LD and haplotype maps. Bioinformatics. 2005;21:263-265.
22. Parker KC, Bednarek MA, Coligan JE. Scheme for ranking potential HLA-A2 binding peptides based on independent binding of individual peptide side-chains. J Immunol. 1994;152:163-175.
23. Kubo RT, Sette A, Grey HM, et al. Definition of specific peptide motifs for four major HLA-A alleles. J Immunol. 1994;152:3913-3924.
24. Dolstra H, de Rijke B, Fredrix H, et al. Bi-directional allelic recognition of the human minor histocompatibility antigen HB-1 by cytotoxic T lymphocytes. Eur J Immunol. 2002;32:2748-2758.
25. Easton DF, Pooley KA, Dunning AM, et al. Genome-wide association study identifies novel breast cancer susceptibility loci. Nature. 2007;447:1087-1093.
26. Gudmundsson J, Sulem P, Manolescu A, et al.

Genome-wide association study identifies a second prostate cancer susceptibility variant at 8q24. Nat Genet. 2007;39:631-637.

27. Zeggini E, Weedon MN, Lindgren CM, et al. Replication of genome-wide association signals in UK samples reveals risk loci for type 2 diabetes. Science. 2007;316:1336-1341.
28. Su AI, Cooke MP, Ching KA, et al. Large-scale analysis of the human and mouse transcriptomes. Proc Natl Acad Sci U S A. 2002;99:4465-4470.
29. Nannya Y, Taura K, Kurokawa M, Chiba S, Ogawa S. Evolution of genome-wide power of genetic association studies based on empirical data from the HapMap project. Hum Mol Genet. 2007;16:3494-3505.
30. Spierings E, Brickner AG, Caldwell JA, et al. The minor histocompatibility antigen HA-3 arises from differential proteasome-mediated cleavage of the lymphoid blast crisis (Lbc) oncoprotein. Blood. 2003;102:621-629.
31. Brickner AG, Warren EH, Caldwell JA, et al. The immunogenicity of a new human minor histocompatibility antigen results from differential antigen processing. J Exp Med. 2001;193:195-206.
32. Kloosterboer FM, van Luxemburg-Heijs SA, van Soest RA, et al. Minor histocompatibility antigen-specific T cells with multiple distinct specificities can be isolated by direct cloning of IFNgamma-secreting T cells from patients with relapsed leukemia responding to donor lymphocyte infusion. Leukemia. 2005;19:83-90.
33. Tykodi SS, Warren EH, Thompson JA, et al. Allogeneic hematopoietic cell transplantation for metastatic renal cell carcinoma after nonmyeloablative conditioning: toxicity, clinical response, and immunological response to minor histocompatibility antigens. Clin Cancer Res. 2004;10:7799-7811.
34. Kenny JJ, Knobloch TJ, Augustus M, Carter KC, Rosen CA, Lang JC. GRS, a novel member of the Bcl-2 gene family, is highly expressed in multiple cancer cell lines and in normal leukocytes. Oncogene. 1997;14:997-1001.

European Journal of Haematology ISSN 0902-4441

ORIGINAL ARTICLE

Low absolute lymphocyte count is a poor prognostic marker in patients with diffuse large B-cell lymphoma and suggests patients' survival benefit from rituximab

Yasuhiro Oki, Kazuhito Yamamoto, Harumi Kato, Yachiyo Kuwatsuka, Hirofumi Taji, Yoshitoyo Kagami, Yasuo Morishima

Department of Hematology and Cell Therapy, Aichi Cancer Center Hospital, Nagoya, Japan

Abstract

Objectives: To evaluate the prognostic value of absolute lymphocyte count (ALC) at diagnosis in patients with diffuse large B-cell lymphoma (DLBCL). *Methods:* In a large cohort of patients with DLBCL treated with CHOP (n = 119) or RCHOP (n = 102) in our institution, we evaluated the prognostic value of ALC at diagnosis with regards to treatment response, overall (OS) and progression-free survival (PFS). Use of rituximab, all International Prognostic Index (IPI) determinants, β2microglobulin level, presence of B symptoms or bulky disease, and ALC were evaluated. *Results:* Low ALC ($<1.0 \times 10^9$/L) was associated with advanced stage, performance status ≥2, elevated lactate dehydrogenase, number of extranodal involvement ≥2, B symptoms, elevated β2microglobulin and higher IPI risk group. Low ALC was associated with lower CR rate by univariate analysis (odds ratio = 3.29, P = 0.024) but not by multivariate analysis. By univariate analysis using Cox proportional hazard model, low ALC was associated with shorter OS [hazard ratio (HR) = 2.89, $P < 0.001$] and PFS (HR = 2.91, $P < 0.001$). Multivariate analysis revealed that low ALC was associated with shorter OS (HR = 2.51, P = 0.003) and PFS (HR = 2.72, $P < 0.001$), independent of above-mentioned parameters. Subclass analyses revealed that the use of rituximab improves OS in patients with low ALC (HR = 0.42, P = 0.05) but not in those with high ALC (HR = 0.83, P = 0.71). This observation was most obvious in patients with higher IPI score. *Conclusion:* Low ALC is a poor prognostic marker in patients with DLBCL and suggests patients' survival benefit from rituximab.

Key words absolute lymphocyte count; diffuse large B-cell lymphoma; prognostic factor; rituximab

Correspondence Yasuhiro Oki, MD, Department of Hematology and Cell Therapy, Aichi Cancer Center Hospital, 1-1 Kanokoden, Chikusa-ku, Nagoya 464-8681, Japan. Tel: +81-52-762-6111; Fax: +81-52-764-2967; e-mail: yooki-tky@umin.ac.jp

Accepted for publication 14 July 2008

doi:10.1111/j.1600-0609.2008.01129.x

Prognostication of patients with diffuse large B-cell lymphoma (DLBCL) is important in determining optimal treatment approaches. Numbers of prognostic factors have been studied, but some require expensive molecular testing and thus not clinically applicable. Inexpensive and readily available prognostic factors are practical and helpful.

Low absolute lymphocyte count (ALC) at diagnosis is associated with poor prognosis in patients with advanced Hodgkin lymphoma (1) as well as follicular lymphoma (2). A recent preliminary study with short follow-up duration also suggested a potential prognostic value of ALC in DLBCL (3). While International Prognostic Index (IPI) is currently the most valuable prognostic indicator in patients with aggressive lymphoma, ALC was not included in the parameters analyzed (4). We performed a retrospective study evaluating the prognostic value of low ALC using our large cohort of patients with DLBCL, about half treated with CHOP and the rest with RCHOP.

Patients and methods

This retrospective study was approved by the institutional review board. We reviewed 221 consecutive newly

diagnosed patients with non-HIV-associated DLBCL who were treated with CHOP (n = 119; before approval of rituximab) or RCHOP (n = 102; after approval) based therapy at Aichi Cancer Center Hospital between January 1999 and January 2007. Age (≤60 or >60), performance status (PS, ≤1 or ≥2), B symptoms (present or absent), stage (≤2 or ≥3), number of extranodal involvement (≤1 or ≥2), bulky disease (largest diameter of the disease ≥10 cm, present or absent) serum lactate dehydrogenase (LDH) levels (normal or elevated), ALC at diagnosis, IPI group (scored from 0 to 5 by age >60, stage ≥3, PS ≥2, LDH higher than upper limit of normal range and number of extranodal involvement ≥2, and risk groups were classified as low by score 0/1, low-intermediate by score 2, high-intermediate by score 3 and high by score 4/5), initial treatment (CHOP or RCHOP) were collected and incorporated as potential prognostic factors in various analyses. Serum β2microglobulin level was collected if available but excluded from the survival analyses because of many missing data.

The Fisher exact tests were used for the descriptive statistical analyses on categorical data. Overall survival (OS) and progression free survival (PFS, time from diagnosis to disease progression, relapse or death of any cause) were calculated using Kaplan–Meier method (5) and was compared between two groups by log-rank test. Logistic regression models were used to evaluate the associations between multiple characteristics and complete response (CR). Patient characteristics were also analyzed for their association with PFS and OS using Cox proportional hazard models. In this model, characteristics with P-values <0.10 in the univariate analyses were included in the multivariate analyses, and a backward elimination with a P-cutoff of 0.05 was used. All computations were performed in STATA version 9.0 (StataCorp, College Station, TX, USA).

Results

Patient characteristics

Patient characteristics are summarized in Table 1. There was no significant difference in baseline characteristics between CHOP and RCHOP group. In patients with early-stage non-bulky disease, involved field radiation therapy was performed following three courses of CHOP (n = 37) or RCHOP (n = 38) therapy. Patients younger than 65 with age-adjusted IPI score of 2 or 3 were generally offered an option of upfront autologous stem cell transplantation after induction therapy, and 20 such patients (11 after CHOP and nine after RCHOP) underwent this treatment.

The median value of ALC of entire population was 1.20×10^9/L (range 0.10–4.64 $\times 10^9$/L). ALC was significantly higher in IPI low risk (median ALC 1.49×10^9/L), and the values were not significantly different among low-intermediate (median 0.97×10^9/L), high-intermediate (median 0.93×10^9/L) and high-risk (median 0.83×10^9/L) groups (Fig. 1). Low ALC [$< 1.2 \times 10^9$/L (median value)] was associated with advanced stage, PS ≥2, elevated LDH, number of extranodal involvement ≥2, B symptoms, elevated β2microglobulin and higher IPI risk group. Using different cutoff value of ALC (0.8, 1.0 and 1.4×10^9/L) revealed essentially the same result (data using the cutoff value of 1.0×10^9/L are shown in Table 1).

Treatment response

Response to initial treatment was evaluable in 210 patients, among whom CR rate was 91.9%. CR rates in patients with low and high ALC after CHOP were 85.0% (34/40) and 97.3% (72/74), respectively (P = 0.021). Those after RCHOP were 87.5% (35/40) and 92.9% (52/56), respectively (P = 0.483). Univariate analysis using logistic regression model for the chance of achieving CR revealed that elevated LDH, PS ≥2, number of extranodal involvement ≥2 and presence of B symptoms were significantly associated with lower chance of achieving CR. Low ALC [$< 1.2 \times 10^9$/L (median value)] was not significantly associated with low CR rate {odds ratio of low ALC ($< 1.2 \times 10^9$/L) = 2.63 [95% confidence interval (CI) 0.894–7.77], P = 0.079}. Other cutoff values (0.8, 1.0 and 1.4×10^9/L) were also tested in association with CR rate, and the association was significant when cutoff value of 1.0×10^9/L was used [odds ratio of low ALC ($< 1.0 \times 10^9$/L) for low CR rate = 3.29 (95% CI 1.17–9.30), P = 0.024]. The cutoff value of 1.0×10^9/L was also found to be optimal in the survival analyses as shown later. Higher IPI risk group was also associated with lower CR rate [RR = 1.68 (1.11–2.55), P = 0.014]. Multivariate analysis revealed that only PS ≥2 [RR = 5.47 (1.87–16.0), P = 0.002] and elevated LDH [RR = 4.66 (1.25–17.3), P = 0.022] were independently associated with lower CR rate.

Overall survival

The median follow-up duration in the entire population, CHOP and RCHOP groups were 47, 67 and 29 months, respectively. Two-year OS rates in CHOP and RCHOP groups were 82.1 ± 3.6% and 87.0 ± 3.7%, respectively. The Kaplan–Meier OS estimate curves were first plotted according to ALC groups (<0.61, 0.61–0.80, 0.81–1.00, 1.01–1.20, 1.21–1.40, 1.41–1.60 and $> 1.60 \times 10^9$/L) to find the optimal cutoff value to define low and high ALC groups. This revealed that OS was generally longer in patients with higher ALC and curves

Table 1 Patient characteristics

Parameters	*n* (total 221)	ALC < 1.0×10^9/L	*P*-value	Rituximab	*P*-value
All	221	86		102	
Age (yr)					
≤60	106	37	0.270	47	0.686
>60	115	49		55	
Stage					
1/2	136	35	<0.001	62	0.890
3/4	85	51		40	
PS					
0/1	184	62	0.001	85	1.000
≥2	37	24		17	
LDH					
Normal	119	29	<0.001	51	0.344
High	102	57		51	
Number of extranodal involvement					
0/1	177	58	<0.001	83	0.736
≥2	44	28		19	
B symptoms					
Absent	188	65	0.003	84	0.346
Present	33	21		18	
IPI					
Low	117	26	<0.001	50	0.508
Low-intermediate	37	19		20	
High-intermediate	36	21		19	
High	31	20		13	
Bulky disease (≥10 cm)					
No	202	79	1.000	90	0.150
Yes	19	7		12	
Serum β2microglobulin					
<3.0 mg/dL	98	33	0.036	43	0.683
≥3.0 mg/dL	32	18		16	
NA	91	35		43	
Treatment					
CHOP	119	42	0.269	0	–
RCHOP	102	44		102	
ALC					
$<1.0 \times 10^9$/L	86	86	–	44	0.269
$\geq 1.0 \times 10^9$/L	135	0		58	

PS, Eastern Cooperative Oncology Group Performance Status; LDH, serum lactate dehydrogenase level; B symptoms, presence of at least one of the followings – night sweat, weight loss >10% over 6 months and recurrent fever >38.3°C; IPI, International Prognostic Index; ALC, absolute lymphocyte count; NA, not available.
P-values were calculated by Fisher exact test.

were grossly separated at a cutoff value of 1.0×10^9/L (data not shown). To confirm the optimal cutoff values for determining 'low ALC', we next performed sensitivity analysis, where among candidate cutoff values of 0.8, 0.9, 1.0, 1.1, 1.2, 1.3 and 1.4×10^9/L, the maximal hazard ratio (HR) was produced with the cutoff value of 1.0×10^9/L [HR = 2.89 (95% CI 1.61–5.17)]. Low ALC was thus defined to be $< 1.0 \times 10^9$/L for further survival analyses. The Kaplan–Meier OS estimate curves, calculated according to treatment (CHOP and RCHOP) and ALC (high and low) are shown in Fig. 2A. In CHOP group, 2-yr OS rates in patients with high and low ALC were 90.7 ± 3.6% and 66.5 ± 7.3%, respectively. Those in RCHOP group were 92.1 ± 3.8% and 79.8 ± 7.0%, respectively. By univariate analysis using Cox proportional hazard model, low ALC was associated with shorter OS duration in the entire population [HR = 2.89 (1.61–5.17), $P < 0.001$] or in CHOP group [HR = 3.61 (1.81–7.20), $P < 0.001$] but the difference was not significant in RCHOP group [HR = 1.78 (0.599–5.32), $P = 0.298$].

Multivariate analysis for OS incorporating all the characteristics except IPI risk group revealed that PS ≥2 [HR = 3.34 (1.82–6.15), $P < 0.001$], low ALC [HR = 2.51 (1.38–4.58), $P = 0.003$] were independently associated with shorter OS. In this model, rituximab was forced in the analysis [HR = 0.530 (0.276–1.02), $P = 0.057$]. Furthermore, when IPI risk group (analyzed

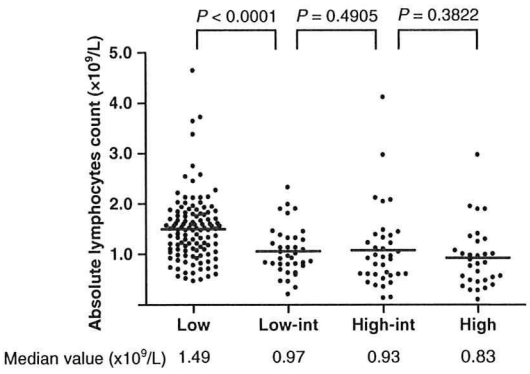

Figure 1 Absolute lymphocyte count according to IPI risk group.) *P*-values were calculated by non-parametric non-paired *t*-test (Man-Whitney test).

as a linear parameter) was incorporated instead of five IPI factors (i.e. age, PS, LDH, stage and number of extranodal involvement were omitted), low ALC was associated with shorter OS [HR = 2.11 (1.12–3.95), P = 0.019], along with IPI group [HR 1.50 (1.16–1.92), P = 0.002], where rituximab was again forced in the model [HR = 0.531 (0.278–1.02), P = 0.056, Table 2]. Removing rituximab from the final model showed the similar result for both analyses. Analyzing IPI risk group as a categorical parameter also showed essentially the same result [HR of low ALC = 2.05 (1.09–3.86), P = 0.026, Table 2].

Given that the baseline patient characteristics were similar in CHOP and RCHOP group (Table 1), OS was next compared between CHOP and RCHOP groups, according to ALC group. Use of rituximab was associated with longer OS in low ALC group [HR = 0.42 (0.18–1.00), P = 0.05] but not in high ALC group [HR = 0.83 (0.31–2.21), P = 0.71]. This suggests that the prognostic significance of ALC became smaller in the era of rituximab, as shown earlier, because the absolute survival benefit from rituximab is larger in low ALC group than in high ALC group (Fig. 2A). To further evaluate the significance of ALC and rituximab use, we next performed subgroup analyses of OS based on IPI risk group (Fig. 2B,C). In this analyses, we defined two IPI risk group [score '0–1' (n = 117) and '2–5' (n = 104)] because of significantly higher ALC distribution only in '0–1' group (Fig. 1), and limited number of patients in each low-intermediate, high-intermediate and high-risk group. The use of rituximab in patients with IPI '2–5' group with low ALC was associated with longer OS [HR = 0.35 (0.12–0.98), P = 0.045], but not in IPI '2–5' with high ALC [HR = 1.02 (0.33–3.13), P = 0.978], or in IPI '0–1' with low ALC [HR = 0.83 (0.15–4.44), P = 0.824] or in IPI '0–1' with high ALC [HR = 0.42 (0.05–3.67), P = 0.432].

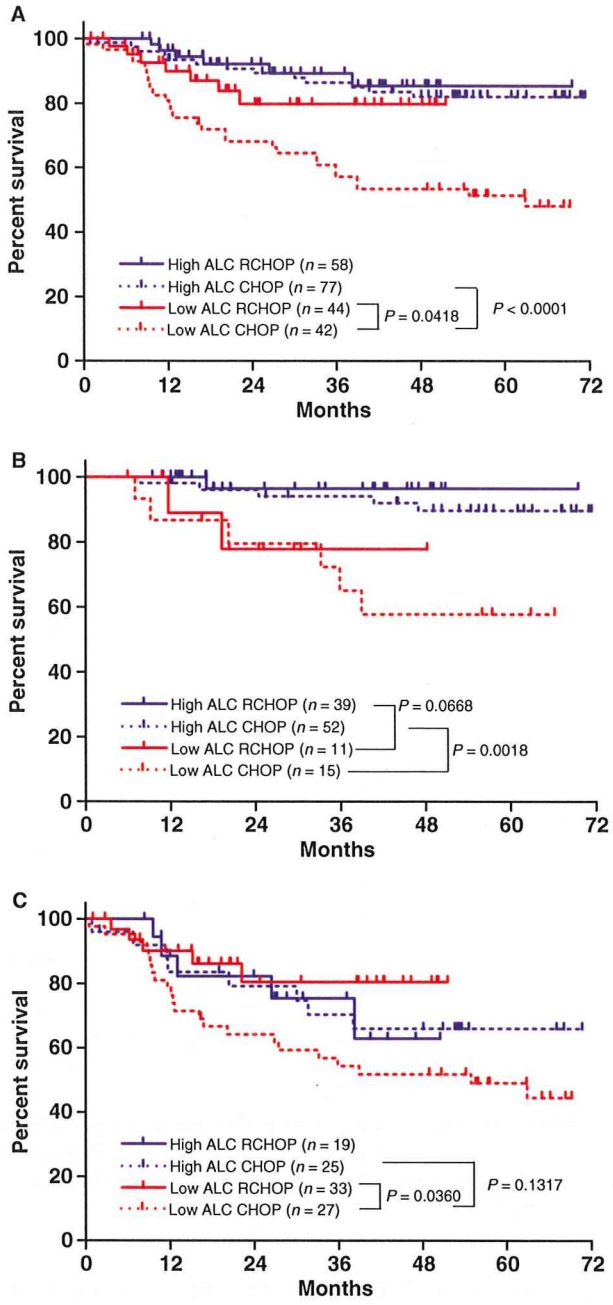

Figure 2 Overall survival according to absolute lymphocyte count and use of rituximab.) (A) All patients; (B) IPI score 0–1; (C) IPI score 2-5. *P*-values were calculated by Log-rank test. *P*-value for any survival comparison was >0.1 if not shown.

Progression free survival

We also performed analyses for PFS. Two-year PFS rates in CHOP group and RCHOP group were 72.8 ± 4.1% and 81.2 ± 4.2%, respectively. In CHOP group, 2-yr PFS rates in high and low ALC groups were 82.8 ± 4.3% and 54.6 ± 7.7%, respectively. In RCHOP group, those were

Table 2 The result of multivariate analyses for OS and PFS when IPI group was analyzed either as a linear parameter or a categorical parameter.

	Hazard ratio	95% CI	*P*-value
For OS			
Low ALC (<1.0 × 10^9/L)	2.11	1.12–3.95	0.019
IPI as a linear parameter	1.50	1.16–1.92	0.002
Rituximab (forced in the model)	0.531	0.278–1.02	0.056
For OS			
Low ALC (<1.0 × 10^9/L)	2.05	1.09–3.86	0.026
IPI			
Low-intermediate vs. low	1.93	0.831–4.49	0.126
High-intermediate vs. low	1.29	0.511–3.27	0.588
High vs. low	3.26	1.19–7.11	0.003
B symptoms	2.37	1.16–4.83	0.018
Rituximab	0.471	0.243–0.915	0.026
For PFS			
Low ALC (<1.0 × 10^9/L)	2.17	1.25–3.76	0.006
IPI as a linear parameter	1.53	1.22–1.91	<0.001
Rituximab	0.452	0.255–0.801	0.007
For PFS			
Low ALC (<1.0 × 10^9/L)	2.22	1.28–3.87	0.005
IPI			
Low-intermediate vs. low	1.52	0.703–3.28	0.287
High-intermediate vs. low	1.72	0.813–3.62	0.156
High vs. low	3.80	1.95–7.44	<0.001
Rituximab	0.457	0.258–0.810	0.007

84.0 ± 5.3% and 77.8 ± 6.6%, respectively. By univariate analysis using Cox proportional hazard model, low ALC was associated with shorter EFS duration in the entire population [HR = 2.91 (1.75–4.86), $P < 0.001$] or in CHOP group [HR = 3.90 (2.12–7.16), $P < 0.001$] but the difference was not significant in RCHOP group [HR = 1.68 (0.647–4.35), $P = 0.287$]. Multivariate analysis for PFS incorporating all characteristics except IPI group revealed that PS ≥2 [HR = 3.40 (1.98–5.83), $P < 0.001$], low ALC [HR = 2.72 (1.61–4.60), $P < 0.001$] and rituximab [HR = 0.433 (0.242–0.772), $P = 0.005$] were independently associated with shorter PFS. When IPI group as a linear parameter was incorporated instead of five IPI factors, low ALC was again associated with shorter PFS [HR = 2.17 (1.25–3.76), $P = 0.006$], along with IPI group [HR 1.53 (1.22–1.91), $P < 0.001$] and rituximab [HR = 0.452 (0.255–0.801), $P = 0.007$, Table 2]. Analyzing IPI risk group as a categorical parameter also showed similar result [HR of low ALC = 2.22 (1.28–3.87), $P = 0.005$, Table 2].

Discussion

ALC is an objective and reproducible test result, which can be obtained by basic laboratory equipment. Our study demonstrated that low ALC is a poor prognostic factor with regards to OS and PFS. Such prognostic value of ALC is in agree with other recently published studies (3, 6, 7). Although the actual mechanisms of this association between low ALC and poor prognosis is unclear, possibilities include: (i) low ALC may be associated with already immunosuppressed condition, suggesting that the host tends to have an inadequate immunological reaction; (ii) low ALC may be a consequence of lympholytic cytokines produced by lymphoma cells, and such lymphoma may already have a resistant character by itself; or (iii) the combination of these two or other.

The prognostic value of ALC was most remarkable in patients treated with CHOP without rituximab. The difference of prognostic impact between CHOP and RCHOP groups is largely because of the improvement of survival by rituximab in patients with low ALC. Particularly in the group of IPI score 2–5, treatment with rituximab significantly improved survival of patients with low ALC, but not significantly that of patients with high ALC. Analogy of this prognostic value of low ALC is that of expression of BCL2, which was a significant poor prognostic indicator before the emergence of rituximab but not in the era of rituximab (8).

Obvious limitation of this comparison is that salvage regimens might or might not have contained rituximab in relapsed patients in CHOP group (although this would not affect OS), and that the patients were not randomized (although characteristics shown in Table 1 were similar in the two groups). Although not using rituximab in addition to CHOP in any patients with DLBCL may not be justifiable given the little toxicity and significant potential benefit (9, 10), it should be noted that the absolute survival benefit is likely larger in patients with low ALC than in those with high ALC, in the era of multiple target therapy agents (currently approved or not) which may lead to expanding costs with significant impact on the economy.

Acknowledgements

We thank Ryoko Yamauchi and Aki Kobayashi for their excellent secretarial support.

Conflict of interest

None.

Authors' contributions

All authors contributed to the patient care and data collection. Y. O. designed the study, analyzed data and wrote the paper. K. Y. analyzed the data and edited the paper. H. K. and Y. Kuwatsuka edited the paper. H. T. and Y. Kagami reviewed the paper. Y. M. supervised the patient care and edited the paper.

References

1. Hasenclever D, Diehl V. A prognostic score for advanced Hodgkin's disease. International Prognostic Factors Project on Advanced Hodgkin's Disease. *N Engl J Med* 1998;**339**:1506–14.
2. Siddiqui M, Ristow K, Markovic SN, *et al.* Absolute lymphocyte count predicts overall survival in follicular lymphomas. *Br J Haematol* 2006;**134**:596–601.
3. Kim DH, Baek JH, Chae YS, Kim YK, Kim HJ, Park YH, Song HS, Chung JS, Hyun MS, Sohn SK. Absolute lymphocyte counts predicts response to chemotherapy and survival in diffuse large B-cell lymphoma. *Leukemia* 2007;**21**:2227–30.
4. The International Non-Hodgkin's Lymphoma Prognostic Factors Project. A predictive model for aggressive non-Hodgkin's lymphoma. *N Engl J Med* 1993;**329**:987–94.
5. Kaplan EL, Meire P. Nonparametric estimation from incomplete observations. *J Am Stat Assoc* 1958;**53**:457–81.
6. Cox MC, Nofroni I, Laverde G, *et al.* Absolute lymphocyte count is a prognostic factor in diffuse large B-cell lymphoma. *Br J Haematol* 2008;**141**:265–8.
7. Talaulikar D, Choudhury A, Shadbolt B, Brown M. Lymphocytopenia as a prognostic marker for diffuse large B cell lymphomas. *Leuk Lymphoma* 2008;**49**:959–64.
8. Mounier N, Briere J, Gisselbrecht C, *et al.* Rituximab plus CHOP (R-CHOP) overcomes bcl-2 – associated resistance to chemotherapy in elderly patients with diffuse large B-cell lymphoma (DLBCL). *Blood* 2003;**101**:4279–84.
9. Coiffier B, Lepage E, Briere J, *et al.* CHOP chemotherapy plus rituximab compared with CHOP alone in elderly patients with diffuse large-B-cell lymphoma. *N Engl J Med* 2002;**346**:235–42.
10. Pfreundschuh M, Trumper L, Osterborg A, *et al.* CHOP-like chemotherapy plus rituximab versus CHOP-like chemotherapy alone in young patients with good-prognosis diffuse large-B-cell lymphoma: a randomised controlled trial by the MabThera International Trial (MInT) Group. *Lancet Oncol* 2006;**7**:379–91.

De novo CD5+ diffuse large B-cell lymphoma: results of a detailed clinicopathological review in 120 patients

Motoko Yamaguchi,[1] Naoya Nakamura,[2] Ritsuro Suzuki,[3] Yoshitoyo Kagami,[4] Masataka Okamoto,[5] Ryo Ichinohasama,[6] Tadashi Yoshino,[7] Junji Suzumiya,[8] Takuhei Murase,[9] Ikuo Miura,[10] Koichi Ohshima,[11] Momoko Nishikori,[12] Jun-ichi Tamaru,[13] Masafumi Taniwaki,[14] Masami Hirano,[5,15] Yasuo Morishima,[4] Ryuzo Ueda,[16] Hiroshi Shiku,[1] and Shigeo Nakamura[1]

[1]Mie University Graduate School of Medicine, Tsu; [2]Tokai University, Isehara; [3]Nagoya University Graduate School of Medicine, Nagoya; [4]Aichi Cancer Center, Nagoya; [5]Fujita Health University School of Medicine, Toyoake; [6]Tohoku University Postgraduate School of Medicine, Sendai; [7]Okayama University Graduate School of Medicine and Dentistry, Okayama; [8]Fukuoka University Chikushi Hospital, Fukuoka; [9]Nishio Municipal Hospital, Nishio; [10]St. Marianna Medical University, Kawasaki; [11]Kurume University School of Medicine, Kurume; [12]Kyoto University, Kyoto; [13]Saitama Medical Center, Kawagoe; [14]Kyoto Prefectural University of Medicine, Kyoto; [15]Meijo University, Nagoya, and [16]Nagoya City University Medical School, Nagoya, Japan

Acknowledgments: we thank the collaborators from the institutions for providing patients' data and specimens. A list of participating institutes is given in the Appendix. This paper was presented in part at the 49th Annual Meeting of the American Society of Hematology, Atlanta, December 2007.

Funding: this work was supported in part by Grants-in-Aid for Cancer Research (15-11, 19-8) from the Ministry of Health, Labour and Welfare, Japan.

Manuscript received January 24, 2008. Revised version arrived on March 26, 2008. Manuscript accepted April 15, 2008.

Correspondence:
Motoko Yamaguchi, M.D., Ph.D., Department of Hematology and Oncology, Mie University Graduate School of Medicine, 2-174 Edobashi, Tsu, Mie 514-8507, Japan.
E-mail: waniwani@clin.medic.mie-u.ac.jp

ABSTRACT

Background

De novo CD5-positive diffuse large B-cell lymphoma (CD5+ DLBCL) is clinicopathologically and genetically distinct from CD5-negative (CD5-) DLBCL and mantle cell lymphoma. The aim of this retrospective study was to clarify the histopathological spectrum and obtain new information on the therapeutic implications of CD5+ DLBCL.

Design and Methods

From 1984 to 2002, 120 patients with CD5+ DLBCL were selected from 13 collaborating institutes. We analyzed the relationship between their morphological features and long-term survival. The current series includes 101 patients described in our previous study.

Results

Four morphological variants were identified: common (monomorphic) (n=91), giant cell-rich (n=13), polymorphic (n=14), and immunoblastic (n=2). Intravascular or sinusoidal infiltration was seen in 38% of the cases. BCL2 protein expression in CD5+ DLBCL was more frequent than in CD5- DLBCL (p=0.0003). Immunohistochemical analysis in 44 consecutive cases of CD5+ DLBCL revealed that 82% of these cases (36/44) were non-germinal center B-cell type DLBCL. The 5-year overall survival rate of the patients with CD5+ DLBCL was 38% after a median observation time of 81 months. Patients with the common variant showed a better prognosis than those with the other three variants (p=0.011), and this was confirmed on multivariate analysis. Overall, 16 patients (13%) developed central nervous system recurrence.

Conclusions

Our study revealed the morphological spectrum of CD5+ DLBCL, found that the incidence of central nervous system recurrence in this form of lymphoma in high, confirmed that CD5+ DLBCL frequently expresses BCL2 protein and showed that it is mainly included in the non-germinal center B-cell type of DLBCL.

Key words: diffuse large B-cell lymphoma, CD5, histopathology, BCL2, central nervous system.

Citation: Yamaguchi M, Nakamura N, Suzuki R, Kagami Y, Okamoto M, Ichinohasama R, Yoshino T, Suzumiya J, Murase T, Miura I, Ohshima K, Nishikori M, Tamaru J, Taniwaki M, Hirano M, Morishima Y, Ueda R, Shiku H and Nakamura S. De novo CD5+ diffuse large B-cell lymphoma: results of a detailed clinicopathological review in 120 patients. Haematologica 2008; 93:1195-1202. doi: 10.3324/haematol.12810

Introduction

Diffuse large B-cell lymphoma (DLBCL) constitutes the largest category of aggressive lymphomas, and is considered to have heterogeneous biological properties.[1,2] The phenomenon of CD5 expression in DLBCL evolving *de novo*, and not as a result of the transformation of chronic lymphocytic leukemia and mantle cell lymphoma, was first described by Matolcsy *et al.* in 1995.[3] Since then, accumulating clinicopathological evidence has gradually clarified that *de novo* CD5-positive ($CD5^+$) DLBCL constitutes a unique subgroup of DLBCL.[4-13] *De novo* $CD5^+$ DLBCL is associated with onset in old age, female predominance, advanced stage at diagnosis, the presence of B symptoms, high levels of lactate dehydrogenase, and the frequent involvement of extranodal sites. The genetic analysis of this lymphoma has suggested that it may originate from somatically mutated $CD5^+$ progenitor B cells.[5,6,8,13] Moreover, an analysis using cDNA microarray and comparative genomic hybridization technology demonstrated that *de novo* $CD5^+$ DLBCL is distinct from $CD5^-$ DLBCL and mantle cell lymphoma.[12,14-17] Cytogenetic analysis identified a subgroup of patients with *de novo* $CD5^+$ DLBCL with chromosomal abnormalities in 8p21 or 11q13 who have a poor prognosis.[18]

We reported that *de novo* $CD5^+$ DLBCL tumors usually show a centroblastic morphology, and 19% show an intravascular or sinusoidal growth pattern.[11] However, CD5 is expressed in some cases of intravascular large B-cell lymphoma[19-22] and T-cell-rich B-cell lymphoma,[23] and cases of $CD5^+$ follicular lymphoma[24,25] and $CD5^+$ Burkitt's lymphoma[26] have been reported. The relationship between these tumors and *de novo* $CD5^+$ DLBCL remains to be clarified. We reported that *de novo* $CD5^+$ DLBCL shows an aggressive clinical course, with a 5-year overall survival rate of 34%.[11] However, the median observation period in our previous study was 33 months; the results should, therefore, be confirmed by long-term survival analysis.

To clarify the histopathological spectrum of $CD5^+$ DLBCL and obtain new information on the therapeutic implications, we performed a detailed clinicopathological review and long-term follow-up analysis in a larger number of patients with *de novo* $CD5^+$ DLBCL.

Design and Methods

Patients

We selected 120 patients with *de novo* $CD5^+$ DLBCL from 13 collaborating institutes. All patients were diagnosed between 1984 and 2002 as having DLBCL according to the WHO classification,[2] and they had no past history of any other lymphoproliferative disorders. All specimens for histological and immunophenotypic studies were obtained at the initial presentation of the patients, and were examined for CD5 antigen expression by means of flow cytometry and/or immunohistochemistry. All patients were immunohistochemically confirmed to be cyclin D1-negative. The current series includes 101 of 109 *de novo* $CD5^+$ DLBCL cases described in our previous study.[11] Seven patients who fulfilled the diagnostic criteria for intravascular large B-cell lymphoma[2] and one patient with follicular colonization were excluded. The study was approved by the Ethics Committee of Mie University Graduate School of Medicine, and complied with the Helsinki Declaration.

Clinical information was obtained from the hospital records or supplied by the physicians at the collaborating centers.

Morphological evaluation

Tissue was fixed in 10% formalin and embedded in paraffin. Sections (5 μm thick) were stained with hematoxylin and eosin. We examined all the 120 initial diagnostic specimens of the *de novo* $CD5^+$ DLBCL cases, consisting of 85 lymphatic tissues such as lymph node, Waldeyer's ring, and spleen and 35 extranodal tissues with lymphomatous involvement. All cases were blindly reviewed twice by three of the authors (*MY, NN, and SN*). If discrepancies occurred, we discussed the cases while using a multiheaded microscope to reach a consensus.

Immunophenotypic study

Immunohistochemical and flow-cytometric analyses were performed as described previously.[27,28] The monoclonal antibodies used were Leu4 (CD3), Leu1 (CD5), and CALLA (CD10) (Becton Dickinson, Mountain View, CA, USA); J5 (CD10) and B1 (CD20) (Coulter, Hialeah, FL, USA); H107 (CD23) (Nichirei, Tokyo, Japan); MHM6 (CD23), BerH2 (CD30), UCHL1 (CD45RO), HM57 (CD79a), anti-immunoglobulin (Ig)G, anti-IgA, anti-IgM, anti-IgD, anti-kappa, and anti-lambda (DAKO, Carpentaria, CA, USA); 4C7 (CD5) and NCL-CD10 (CD10) (Novocastra, Newcastle, UK), and cyclin D1 (IBL, Gunma, Japan). More than 20% positivity of the tumor cells was considered to indicate positivity for the purposes of this study. Based on preliminary data that the incidence of CD5 positivity in DLBCL examined with paraffin material is approximately half of that examined using frozen sections, and that it can be increased using more sensitive immunohistochemical methods (*Yamaguchi M et al., presented at the Annual Meeting of the Japanese Society of Lymphoreticular Tissue Research, 2000*), CD5 expression was examined primarily by flow cytometry and/or immunohistochemistry in the frozen sections from 104 cases of *de novo* $CD5^+$ DLBCL. In the remaining 16 cases, CD5 expression was examined immunohistochemically using paraffin-embedded sections. In fact, 75% or more of the neoplastic cells were confirmed to be positive for CD5 in the cases examined using paraffin-embedded material alone.

BCL2 protein expression was examined by means of immunohistochemistry using paraffin sections and a monoclonal antibody (BCL2, DAKO). Paraffin-embedded material for this study was available in 96 out of 120 cases. Staining for BCL2 was performed at the Aichi Cancer Center, and the data were compared with those for 150 cases of $CD5^-$ DLBCL, which were sequentially diagnosed at the Aichi Cancer Center during the same period as the *de novo* $CD5^+$ DLBCL cases. The reaction

for BCL2 protein was classified as positive if more than 50% of lymphoma cells were stained.[29]

We also classified *de novo* CD5+ DLBCL into two subgroups, i.e., germinal center B-cell and non-germinal center B-cell types.[30] From the file of histological consultation for diagnosis at the Aichi Cancer Center in the period from 2000 to 2004, 44 cases of *de novo* CD5+ DLBCL were selected for this analysis. Staining for CD10, BCL6 (NCL-BCL6, Novocastra), and MUM1 (MUM1p, DAKO) was performed on paraffin sections.[30] Cases were considered positive if 30% or more of the neoplastic cells were stained with an antibody. Subsequently, each case was classified into germinal center or non-germinal center B-cell types according to the criteria of Hans *et al.*[30]

Statistical analysis

Correlations between the two groups were examined with the χ^2 test and Fisher's exact test. Patients' survival data were analyzed with the Kaplan-Meier method and were compared by means of the log-rank test. Univariate and multivariate analyses were performed with the Cox proportional hazard regression model, and data were analyzed with STATA software (version 9.0, STATA Corp., College Station, TX, USA).

Results

Histopathological review and characterization of morphological variants

At a low magnification, total or partial effacement of the nodal architecture with a diffuse (118 patients, 98%) or vaguely nodular pattern (2 patients, 2%) of tumor cell proliferation was observed. In ten patients (8%), these tumor cells were distributed throughout the interfollicular area, while the follicles which had retained their mantle cuffs were spared.

In the current study, particular attention was paid to the presence or absence of intravascular and/or sinusoidal patterns. Although the extent of such patterns varied in each case, they were seen in 45 cases examined (38%). In the specimens of lymph node obtained from 31 patients, tumor cells infiltrated diffusely and focal intrasinusoidal infiltration was observed simultaneously. In the specimens of bone marrow from seven patients, spleen from two patients, and Waldeyer's ring from one patient, lymphoma cells were observed mainly in the sinusoids. In the other patients, a specimen was taken from the tumor in the nasal cavity, stomach, breast, and testis. In those specimens, lymphoma cells infiltrated diffusely, and focal intravascular infiltration was also observed. There was no significant difference in the incidence of intravascular and/or sinusoidal patterns between lymphatic (34/85, 40%) and extranodal (11/35, 31%) specimens.

The size of tumor cells was medium-to-large in 19 cases, mixed medium and large in 14 cases, and large in 87 cases. The tumor cells generally showed a scant or moderate rim of pale baso- or amphophilic cytoplasm. Of note, bi-nucleated tumor cells with a *snowman-like* morphology were frequently observed in our series (101 out of 120 cases, 85%) (Figures 1A and 2B). Apoptotic cells were observed in 21% of the cases.

We classified *de novo* CD5+ DLBCL according to cytomorphological features (Figure 1). In 91 (76%) of 120 patients, monomorphic proliferation of typical centroblasts was observed, although a few scattered giant cells were seen in nine patients. We regarded these features as the prototype of *de novo* CD5+ DLBCL and referred to it as the common variant. In 13 (11%) out of the remaining patients, there was an increase in very large cells with giant or multiple nuclei, varying from 10 to 30% in area and intermixed with centroblasts and immunoblasts. We referred to this as the giant cell-rich variant. This could correspond to the anaplastic variant of DLBCL according to the WHO classification.[2] While the giant cell-rich variant was thus shown to have a polymorphous composition, monomorphous areas with relatively small cells were also usually identified, suggesting that there is a histological continuum between the common and giant cell-rich variants. CD30 was positive in 23% of the cases (3/13). In 14 patients (12%), tumor cells showed irregularly shaped nuclei,

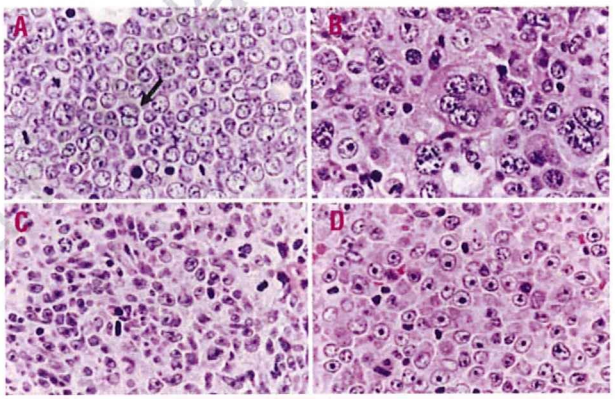

Figure 1. Cytomorphologic features of four variants of *de novo* CD5+ DLBCL. The cells, varying from medium to large in size, are uniform, with a pale basophilic or amphophilic cytoplasm. (A) Common variant, which can be described as the monomorphic or centroblastic variant. *Snowman-like*, bi-nucleated cells were seen (arrow). (B) Giant cell-rich variant. (C) Polymorphic variant, characterized by polymorphous proliferation with medium and large-sized cells. The immunoblastic variant (D) was rare in our case series.

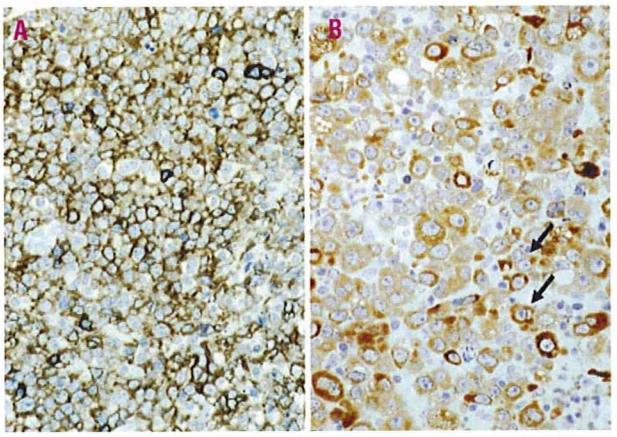

Figure 2. Immunohistochemical features of *de novo* CD5+ DLBCL. Lymphoma cells are positive for CD5 (A) and BCL2 (B). *Snowman-like*, bi-nucleated cells can be seen (arrow).